

Review

Not peer-reviewed version

A Brief Review on Vibration Sensor: Key Parameters, Fundamental Principles, and Recent Progress on Industrial Monitoring Applications

[Limin Ma](#)^{*}, [Zhangpeng Li](#), [Shengrong Yang](#), [Jingjing Wang](#)^{*}

Posted Date: 14 August 2025

doi: 10.20944/preprints202508.1018.v1

Keywords: vibration sensor; fundamental principle; equipment monitoring; future prospects



Preprints.org is a free multidisciplinary platform providing preprint service that is dedicated to making early versions of research outputs permanently available and citable. Preprints posted at Preprints.org appear in Web of Science, Crossref, Google Scholar, Scilit, Europe PMC.

Copyright: This open access article is published under a Creative Commons CC BY 4.0 license, which permit the free download, distribution, and reuse, provided that the author and preprint are cited in any reuse.

Disclaimer/Publisher's Note: The statements, opinions, and data contained in all publications are solely those of the individual author(s) and contributor(s) and not of MDPI and/or the editor(s). MDPI and/or the editor(s) disclaim responsibility for any injury to people or property resulting from any ideas, methods, instructions, or products referred to in the content.

Review

A Brief Review on Vibration Sensor: Key Parameters, Fundamental Principles, and Recent Progress on Industrial Monitoring Applications

Limin Ma ^{1,*}, Zhangpeng Li ^{1,2}, Shengrong Yang ¹ and Jinqing Wang ^{1,*}

¹ State Key Laboratory of Solid Lubrication, Lanzhou Institute of Chemical Physics, Chinese Academy of Sciences, Lanzhou 730000, China

² Qingdao Center of Resource Chemistry & New Materials, Qingdao 266000, China

* Correspondence: malimin@licp.cas.cn (L.M.); jqwang@licp.cas.cn (J.W.)

Abstract

This paper presents a systematic review of vibration sensors and their application in equipment monitoring, aiming to provide a comprehensive reference for both academic research and practical applications in this field. Through the classification of measured parameters and sensing principles, this work endeavors to establish a structured understanding of vibration sensor's working mechanism and deliver an in-depth analysis of their recent research achievements. By integrating practical cases from typical domains, this manuscript comprehensively demonstrates the practical value and application potential of vibration sensors in equipment monitoring, illustrating how these sensors are utilized to detect mechanical failures and enhance the performance and safety of automotive systems. Looking forward, with the rapid advancement of the Internet of Things (IoT) and artificial intelligence (AI) technologies, vibration sensors are anticipated to evolve towards multifunctionalization, miniaturization and intelligenizaion, thereby forming a comprehensive monitoring network that improves overall efficiency and reliability of the mechanical systems.

Keywords: vibration sensor; fundamental principle; equipment monitoring; future prospects

1. Introduction

Vibration, a fundamental physical phenomenon defined by the periodic or non-periodic oscillations of system state parameters around an equilibrium state, pervades all scales of the physical universe. Its manifestations are diverse, ranging from gravitational waves generated by cosmic body oscillations and seismic-induced landslides or tsunamis, to biological rhythms such as heartbeat and quantum-level photon fluctuations [1–3]. Each manifestation is governed by distinct excitation mechanisms, rendering vibration a subject of profound scientific interest and practical significance.

In mechanical systems, vibration exhibits a dual influence on operational stability and functional performance. On the positive side, it serves as the foundation for realizing numerous mechanical functions: vibratory feeders optimize material conveying through the control of vibration parameter; vibration-assisted polishing enhances surface finishing quality by introducing controlled oscillatory motions; and vibration directly determines the screening efficiency and accuracy by regulating the motion state of materials on the sieve surface [4–6]. Conversely, abnormal vibrations often indicate equipment malfunctions: rotor mass unbalance generates periodic centrifugal forces during rotation; shaft misalignment causes uneven bearing loads, accelerating wear and inducing vibrations; joint looseness reduces structural stiffness, amplifying vibratory responses; and friction-induced nonlinear forces give rise to complex dynamic behaviors [7–10]. These highlight the indispensable role of precise vibration measurement and analysis in various engineering disciplines [11].

Vibration sensors, which transduce mechanical vibration into processable signals (typically electrical signals), constitute the cornerstone of vibration measurement technology. Research on

vibration sensing can be traced back to 1920s, when McCollum and Peters first commercialized the resistance-bridge-type vibration sensor (accelerometer) [12]. Subsequently, the invented strain gauge accelerometer further expanded the working range of the vibration sensor (range ± 500 g, NF 4500 Hz). However, these mechanoelectric sensors are limited by low signal-to-noise ratios (SNR), low resonance frequencies, mechanical fragility, and poor temperature stability. The advent of piezoelectric vibration sensors has greatly improved the performance of vibration sensors, enabling the rapid development of related technologies [13].

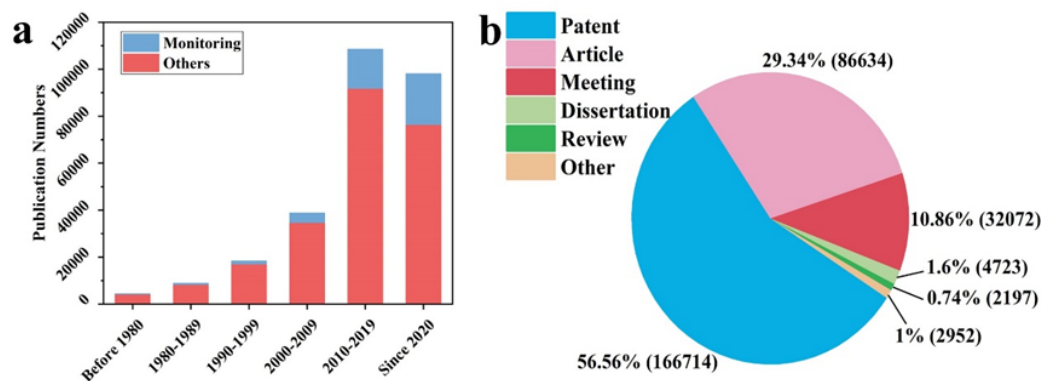


Figure 1. (a) Number of publications filed on vibration sensors and its distribution on monitoring application. (b) The publication types distribution of vibration sensors. (Source: Web of Science with terms “vibration sensor” or “vibration transducer”).

Before 1980s, the annual publication of related documents remained relatively low (Figure 1a). Since the beginning of the 21st century, there has been an evident surge in research reports on vibration sensor. Notably, since 2010, research focusing on vibration sensors for monitoring applications has flourished, emerging as a pivotal research direction within the field. As shown in Figure 2b, more than half of the related publications are patents, indicating that research in vibration sensing is predominantly driven by practical applications. This trend reflects the growing demand for reliable and accurate vibration monitoring solutions across various industries, including aerospace, automotive, manufacturing, and civil engineering. Particularly in mechanical fault diagnosis, assisted with signal processing techniques, vibration signals can accurately identify equipment malfunction and system lubrication conditions, or even predict its fault trend [14,15]. This provides a scientific basis for proactive maintenance, significantly reducing downtime and repair costs.

In recent years, research on vibration sensors has surged, accompanied by a growing number of review papers. These include studies by Babatain et al. focusing on specific parameter monitoring fields such as accelerometers, reviews targeting vibration sensors based on particular sensing mechanisms (e.g., piezoresistive and triboelectric types), and those emphasizing on vibration signal analysis or application [16–21]. However, comprehensive reviews systematically organizing the classification, measurement mechanisms, recent progress and application of vibration sensors are still lacking. Based on the issues mentioned above, this paper presents a systematic review of recent advancements in vibration sensor technologies, detailing their working principles and state-of-the-art developments. Special focus is placed on their applications in mechanical condition monitoring.

2. Key Measurement Parameters for Vibration Sensing

To comprehensively characterize the dynamic behavior of a vibration system, amplitude-related, frequency-related, and energy-related parameters are essential. For complex multi-degree-of-freedom nonlinear vibration systems, vibration modes and their corresponding modal frequencies are equally crucial, as they describe the relative displacement relationships among different system

components during vibration [22]. Currently, the real-time monitoring of vibration behavior in mechanical equipment mainly focuses on sensing and monitoring peak amplitude, vibration frequency, velocity, and acceleration (Figure 2).

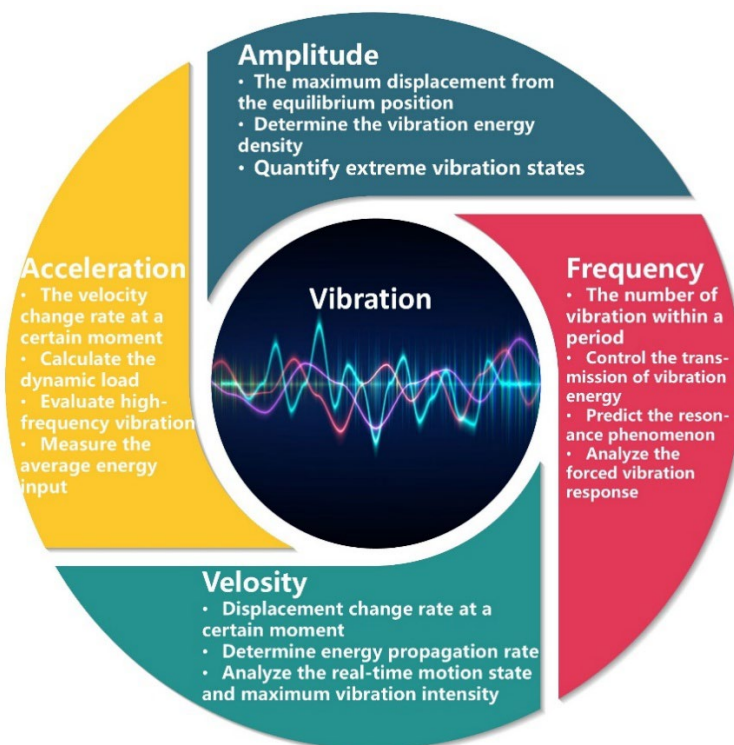


Figure 2. The critical measurement parameters for vibration behavior monitoring.

2.1. Displacement and Amplitude

Displacement is defined as the distance by which a periodic vibrating object deviates from its equilibrium position, while amplitude represents the maximum displacement during vibration and serves as a key indicator of vibration intensity. For the spring-mass simple harmonic vibration system, the total energy (E) is proportional to the square of the amplitude (A), expressed as $E=1/2kA^2$ (where k is the elastic coefficient of the system). In mechanical engineering, larger amplitudes imply more intense energy transfer and exchange during vibration, directly affecting the equipment performance and service life.

For instance, if the vibration amplitude of wind turbine blades exceeds the design standard during rotation, it may lead to a significant increase in transmission loss of wind energy, abnormal temperature rise in the gearbox oil, and premature bearing failure [23]. Similarly, in tunnel excavation, monitoring the vibration amplitude of the shield machine's cutter head is of great importance. Increased cutter head vibration, caused by lubrication failure, uneven slag accumulation, or loose bolts, among other factors, severely compromises operation safety [24]. Amplitude increases during operation often indicate equipment failures or anomalies, such as severe bearing wear or poor gear meshing. Therefore, amplitude is a critical parameter in determining the need for equipment maintenance or repair.

2.2. Frequency

Frequency quantifies the periodicity of vibration. Without external excitation, every vibration system possesses intrinsic characteristic parameters, namely inherent frequencies or natural frequencies (NFs), that reflect its vibrational properties. These NFs are determined by the system's geometric dimensions, material properties, and internal structure. For a spring-mass system, the NF is given by $f_n=1/2\pi\sqrt{(k/m)}$, where m is the mass of the block. When the system is in motion or subjected

to external excitation, its operational vibration frequency is closely related to its motion state and the applied excitation. Bearings, for instance, exhibit complex characteristic NFs influenced by component properties (e.g., elastic modulus, density) and structural parameters (e.g., inner diameter, outer diameter, rolling element diameter, number of rolling elements) [25]. During operation, their vibration frequencies are further affected by rotational speed, ball motion, and cage dynamics, showing diverse operational frequencies.

Resonance occurs when the operational frequency approaches the system's NF, causing a sharp increase in vibration amplitude and potential structural damage [26]. In bridge engineering, for example, vibration frequencies induced by vehicle traffic that approximate the bridge's NF may trigger resonance, threatening the structural safety [27]. In addition, equipment faults alter motion states, causing shifts in its operational frequencies [28]. For example, planetary gearbox fault diagnosis utilizes resonance frequency's speed-independent property and sideband symmetry to extracting fault features from resonance regions [29]. Therefore, accurate frequency measurement can realize operation fault diagnosis and even prediction in equipment monitoring.

2.3. Velocity

Velocity is a physical quantity that describes the instantaneous motion state of a vibrating object. For a vibration system, its energy is primarily composed of kinetic energy (E_k) and potential energy (E_p), i.e., $E = E_k + E_p$. According to the kinetic energy formula $E_k = 1/2mv^2$, the magnitude of velocity directly reflects the E_k of the system. In international standards, the vibration severity levels of equipment are classified according to the root mean square (RMS) value of vibration velocity. Within a vibration system, E_k and E_p are converted into each other during the vibration process. Taking a simple harmonic vibration system as an example, when the mass block moves away from the equilibrium position, the velocity decreases, and the E_k is converted into E_p ($1/2kx^2$, where x is the displacement of the mass block); when moving toward the equilibrium position, the velocity increases, and E_p is converted into E_k , following the relationship $1/2mv^2 + 1/2kx^2 = 1/2kA^2$. In mechanical systems with multi-degree-of-freedom and multi-system interactions, vibration velocity plays a key role in energy transfer processes, affecting the system energy transfer efficiency through wave impedance matching, damping dissipation, modal energy distribution, and nonlinear coupling [30].

Furthermore, changes in vibration velocity can serve as a criterion for evaluating system stability. If the velocity increases without limit due to external interference and lacks effective damping, the system will suffer instability, potentially leading to equipment damage. Li et. al. proposes a noncontact vibration velocity feedback strategy for monitoring active magnetic bearing and demonstrates that velocity feedback enhances low-frequency damping signal [31]. Therefore, the operating status of the equipment can be effectively monitored through changes in vibration velocity.

2.4. Acceleration

Acceleration refers to the change rate of an object's vibration velocity with respect to time, directly reflecting the intensity of vibrational agitation and the magnitudes of dynamic forces acting on the object. Among vibration parameters, acceleration amplitude, representing the maximum value of acceleration during vibration, serves as a critical indicator for evaluating the impact intensity and dynamic loading of vibrations. For instance, in a spring-mass system, the acceleration amplitude (a_{max}) is proportional to the square of the angular frequency (ω) and A , following the relationship $a_{max} = \omega^2 A$. This relationship highlights that acceleration is particularly sensitive to high-frequency vibrational components, making it indispensable for capturing rapid and intense vibrational events.

In mechanical engineering, acceleration amplitude is pivotal for assessing the structural stress, fatigue potential, and dynamic response characteristics of components [32,33]. Higher acceleration amplitudes indicate more severe impact loads and rapid motion state changes during vibration, which significantly affect the structural integrity and operational safety of mechanical systems. For example, Dong et al. proposed a data-driven vibration acceleration prediction method for offshore wind turbine structures based on Harris hawks optimization and extreme gradient boosting [34].

Using 2-month monitoring data from a 3 MW turbine, the optimized model shows high accuracy ($R^2=0.9715$, MAPE=6.55%) and stability in monitoring, with acceptable long-term performance.

3. Principle and Recent Advancements of Vibration Sensors

Vibration sensors play a pivotal role in diverse fields including engineering monitoring, fault diagnosis, and environmental monitoring [30]. They can be categorized through multiple approaches, depending on technical principles, measurement parameters, and application scenarios. Based on different measurement parameters, they are divided into displacement sensors, velocity sensors, and acceleration sensors. This paper primarily focuses on the working principles of vibration sensors, which can be categorized into piezoelectric, piezoresistive, capacitive, electromagnetic, photonic, triboelectric, and hybrid types. From each category, the main challenges and recent research progress of vibration sensors were reviewed and summarized.

3.1. Piezoelectric

Piezoelectric vibration sensors operate based on the piezoelectric effect. In 1880, the Curie brothers discovered that when a quartz crystal is subjected to mechanical stress, its lattice structure deforms, causing the separation of internal positive and negative charge centers [13]. This leads to an imbalance in charge distribution, generating polarized charges on the material surface, which they termed the piezoelectric effect. Since the generated charge is proportional to the applied force, the conversion between mechanical and electrical signals can be achieved. Subsequent research has developed various piezoelectric materials such as lead zirconate titanate (PZT), barium titanate (BTO), polyvinylidene fluoride (PVDF), and other ceramic-matrix and polymer-matrix composites, which have further enriched the system of piezoelectric materials and expanded their sensing application [35,36].

The structure of a piezoelectric vibration sensor typically consists of piezoelectric elements, mass block, circuit system, and base. These sensors boast advantages such as high sensitivity, a broad frequency response range (from several hertz to tens of kilohertz or even higher), self-powered operation, and immunity to electromagnetic interference [14]. They are commonly used in measuring high-frequency vibrations, such as tool vibrations in mechanical processing and engine vibrations in the aerospace. However, limited by the intrinsic properties of traditional piezoelectric materials, piezoelectric sensor devices face challenges in performance enhancement and application expansion.

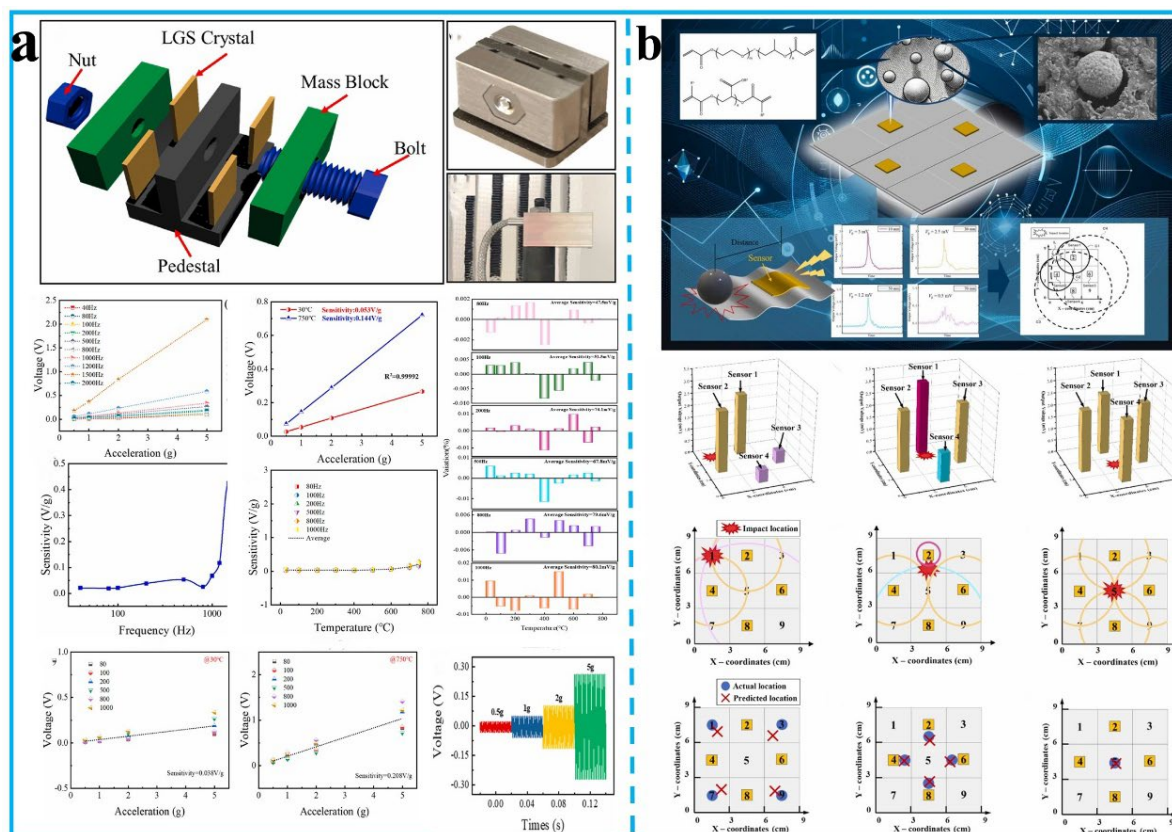


Figure 3. (a) Illustrations of the langasite-based vibration sensor and its vibration sensibility in varied conditions [37]. Reproduced with permission. Copyright 2024, Elsevier. (b) Morphology and composition of BTO piezoelectric composite sensing array and its application performance on impact sensing and locating [38]. Reproduced with permission. Copyright 2024, Elsevier.

The operating temperature of piezoelectric materials is typically below 50% of their Curie temperature (T_c); otherwise, the measurement accuracy degrades or even the functional failure occurs due to property attenuation and phase transitions. For example, the aging rate and relaxation time of PZT at 0.3 T_c were 0.0168 and 213 h, respectively, and turned to 0.0586 and 22 h at 0.8 T_c , due to enhanced vacancy diffusion [39]. Researchers have successively developed high- T_c piezoelectric ceramics such as layered bismuth, alkali metal niobate, and langasite, expanding their application in high temperature equipment monitoring [40–42]. As shown in Figure 3a, Liang et al. developed a shear-type vibration sensor using langasite piezoelectric crystal for high-temperature structural monitoring. Tested across 80–1000 Hz, 0.5–5 g, and 30–750°C, the sensor shows excellent linearity (<1%) and high sensitivity (0.074 V/g). With the decoupling method of temperature and vibration, the maximum error of demodulated acceleration is only 4.54%, making it ideal for aeroengines monitoring.

Charge leakage, caused by the finite resistance of piezoelectric materials and charge amplifiers, makes piezoelectric sensor unable to measure static or ultra-low-frequency vibration (<1 Hz). To this end, researchers have addressed this through material optimization, device structure design, and circuit compensation [43]. Ramany et al. investigated the effect of vanadium doping on the piezoelectric and sensing behaviors of zinc oxide nanorod, finding that 5 wt.% doping achieves 3.528 V/g sensitivity, 77.28% higher than undoped nanorods [44]. Moreover, the doping strategies successfully improved the signal linearity at low-frequency vibration. Ramanathan et al. introduced a differential compensated charge amplifier into sensing system for near-static and low-frequency strain measurements using piezoelectric PVDF films [45]. The sensor achieves a 0.01 mHz–310 kHz sensing range, 95% drift reduction, and 30 dB sensitivity increase with uniaxial near-DC strain measurements stays maintaining <3% voltage over 500 s.

Additionally, to meet the requirements in wearable devices, low-temperature adaptability, and environmental friendliness, extensive research has focused on flexible, lead-free piezoelectric materials [46]. For example, Deng et al. designed a PZT-7A ceramic-based triaxial piezoelectric vibration sensor suitable for low-temperature sensing [47]. Compared to room temperature, its X-, Y-, and Z-axis voltage sensitivities varied by just 1.78%, 2.65%, and 3.33%. As shown in Figure 3b, Narita et al. developed an elastic porous polymer-based piezoelectric composite film with BTO particles for vibration and impact sensing. The film shows excellent flexibility and stability, remaining reliable after 8 million cycles. The sensor exhibited enhanced piezoelectric properties, with direct impact generating a 22 mV output. When assembled into a 4-sensor array combined with the centroid localization algorithm, the device enables accurate impact positioning within a 3×3 grid.

3.2. Electromagnetic

Electromagnetic vibration sensors achieve the perception and conversion of vibration signals based on the electromagnetic induction effect. In 1831, Michael Faraday discovered Faraday's law of electromagnetic induction, laying a theoretical foundation for the development of electromagnetic sensors [48]. The core principle is that when vibration causes relative motion between a magnet and a coil, the coil cuts the magnetic field lines, leading to a change in magnetic flux, thereby generating an induced current or voltage signal in the circuit [49]. The amplitude of the output electrical signal corresponds to parameters such as vibration acceleration and velocity. With the development of electromagnetic science, researchers have developed various magnetic circuit structures and coil designs, enabling the measurement of multiple signals including electromotive force, induced current, and inductance [50,51]. In the field of materials, researchers have successively developed composite magnetic circuit systems such as permanent magnets (e.g., neodymium-iron-boron, samarium-cobalt) and soft magnetic materials (e.g., silicon steel sheets, permalloy), further expanding their applications in different vibration scenarios [52,53].

The structure of electromagnetic vibration sensors typically includes components such as magnetic materials, induction coils, spring-damper systems, and signal conditioning circuits. These sensors possess significant advantages, including high output (usually in the millivolt to volt range), self-power supply, excellent long-term stability, and sensitive response to medium and high-frequency vibrations [54]. They are widely applied in scenarios such as industrial equipment vibration monitoring (e.g., fans, motors), automobile engine vibration detection, and rail transit vibration analysis. However, affected by magnet performance and structural inertia, electromagnetic vibration sensors still have limitations in miniaturized design, soft device, and low-frequency vibration detection.

To address the above issues, Zhao et al. developed a fully flexible electromagnetic Micro-Electro-Mechanical Systems (MEMS) vibration sensor using a suspended flexible magnet enclosed in a multi-layer flexible coil and annular origami magnetic membranes (Figure 4). The annular membranes enhance the overall magnetism by 291% and extend the magnetic field to cover the entire coil region. The sensor exhibits a broad frequency response (1 Hz to 10 kHz) and a sensitivity of 0.59 mV/ μm at 1.7 kHz. Its fully flexible format enables applications in motion detection, voice recognition (with a 98-99% accuracy), biophysical sensing (heart rate, pulse), and machine diagnostics by adapting to complex surfaces. Additionally, it supports wireless transmission and shows potential for battery-less, self-sustainable operation and distributed sensing.

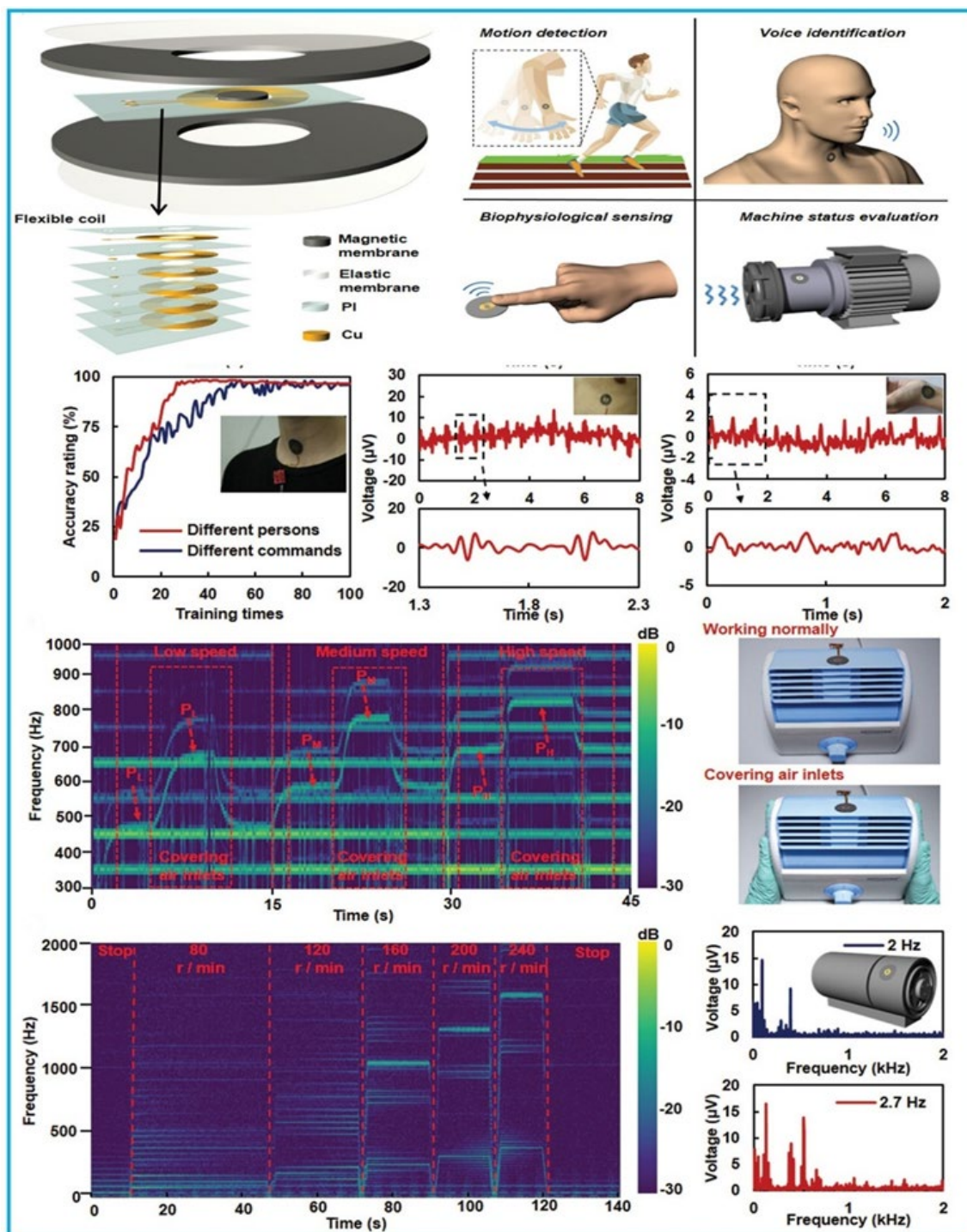


Figure 4. The structure of the fully flexible electromagnetic vibration Sensor and vibration monitoring performances [55]. Copyright 2020, John Wiley and Sons.

3.3. Photonic

Photonic vibration sensors predominantly operate based on photon-related physical phenomena, encompassing the photoelectric effect, Doppler shift, and photon interference [56–58]. Based on their specific operational principles, photonic vibration sensors are further categorized into fiber optic interference-type, laser Doppler-type, photoelectric-type, and so on. Among these categories, the optical fiber-type and laser-type sensors have garnered significant research attention owing to their distinct measurement capabilities and application potentials [59,60].

Fiber optic vibration sensors work on the principle that mechanical vibrations induce micro-deformations in optical fiber waveguides, thereby modulating the intrinsic properties (including phase, intensity, and frequency) of photons propagating through the fiber core. This mechanism enables precise vibration monitoring with exceptional performance metrics, such as ultra-high sensitivity, a broad operational bandwidth spanning multiple frequency and amplitude scales, robust anti-electromagnetic interference capability, and an extended detection range exceeding several kilometers [61,62]. However, inherent limitations persist: pronounced directional dependence in vibration response; fiber degradation induced by intense vibrational stress, elevated temperatures, and high-humidity environments; and relatively high manufacturing and application costs. To address these issues, researchers have developed advanced optical materials, protective coatings, compensation circuits, and integrated modular designs, which collectively reduce measurement deviations [63–65]. Nevertheless, the stringent equipment specifications and consequent high assembly and operational expenses remain critical barriers to their large-scale commercialization.

Laser-based vibration sensors typically leverage the Doppler effect, wherein laser radiation incident upon a vibrating target undergoes frequency or phase shifts in its reflected component, directly correlated with the target's vibrational dynamics [66]. This physical principle enables non-contact vibration measurement with superior precision, where displacement resolution reaches nanometric or even sub-nanometric scales [67]. Moreover, their sensing capacities exhibit a broad displacement and frequency ranges immunity to electromagnetic interference, and extended measurement distances exceeding tens of meters. Such attributes render them indispensable in scenarios requiring non-invasive monitoring, including precision machinery diagnostics and ancient structures assessment [68,69]. Conversely, their performance is significantly influenced by the surface reflectivity of the measured object, susceptibility to ambient light perturbations, and prohibitive equipment costs, which collectively constrain their widespread application [70].

Notably, both fiber optic and laser-based photonic sensors exhibit complementary advantages in specific application scenarios. Fiber optic systems excel in long-distance monitoring and harsh electromagnetic environments, while laser sensors are irreplaceable in non-contact, high-precision measurement tasks. Current research endeavors primarily focus on three directions: material engineering to enhance fiber durability under extreme conditions, adaptive optical systems to compensate for ambient light interference in laser measurements, and cost optimization through miniaturized component integration. Addressing these technical challenges will be pivotal for expanding the practical utility of photonic vibration sensors across industrial, aerospace, and cultural heritage preservation domains.

3.4. Capacitive

Capacitive vibration sensors operate based on the variation of capacitance with mechanical vibration. Originated with the invention of Leyden jar in 1740s, the principles of capacitance were the theoretical foundation for capacitive sensors [71]. The structure of capacitive vibration sensors mainly includes capacitive sensing unit, signal conditioning circuit, and encapsulation structure. As the core component, the capacitive sensing unit can be categorized into different types based on the capacitance variation mechanism, such as changes in electrode spacing, area, and dielectric constant [71]. Among these, the spacing-type and the area-type represent the primary types in current vibration sensors. In particular, the spacing-type is mainstream in industrial applications due to its structural compactness and compatibility with MEMS technology [72]. Besides, capacitive vibration sensors feature high sensitivity, capable of detecting tiny vibration changes (nanometer scale); good linearity, with output signals linearly related to vibration amplitude; fast dynamic response, enabling rapid capture of vibration signal changes [73].

However, capacitive vibration sensors have several limitations. High output impedance and parasitic capacitance lead to rapid signal attenuation, poor SNR, and susceptibility to external interference [74]. These sensors are sensitive to environmental factors such as humidity and temperature, where environmental fluctuations may cause capacitance drift and compromise

measurement accuracy. Furthermore, their structural characteristics result in a trade-off between sensitivity and stability [75]. For instance, reducing the distance between the plates can enhance sensitivity, but this makes the capacitive structure prone to breakdown and reduces stability. Thus, in recent years, researchers have carried out a large amount of research in fields such as materials, processes, structures, circuit, and signal processing [76,77]. At the same time, accuracy, precision, flexibility, linearity, intelligence, and self-powering have also received extensive attention.

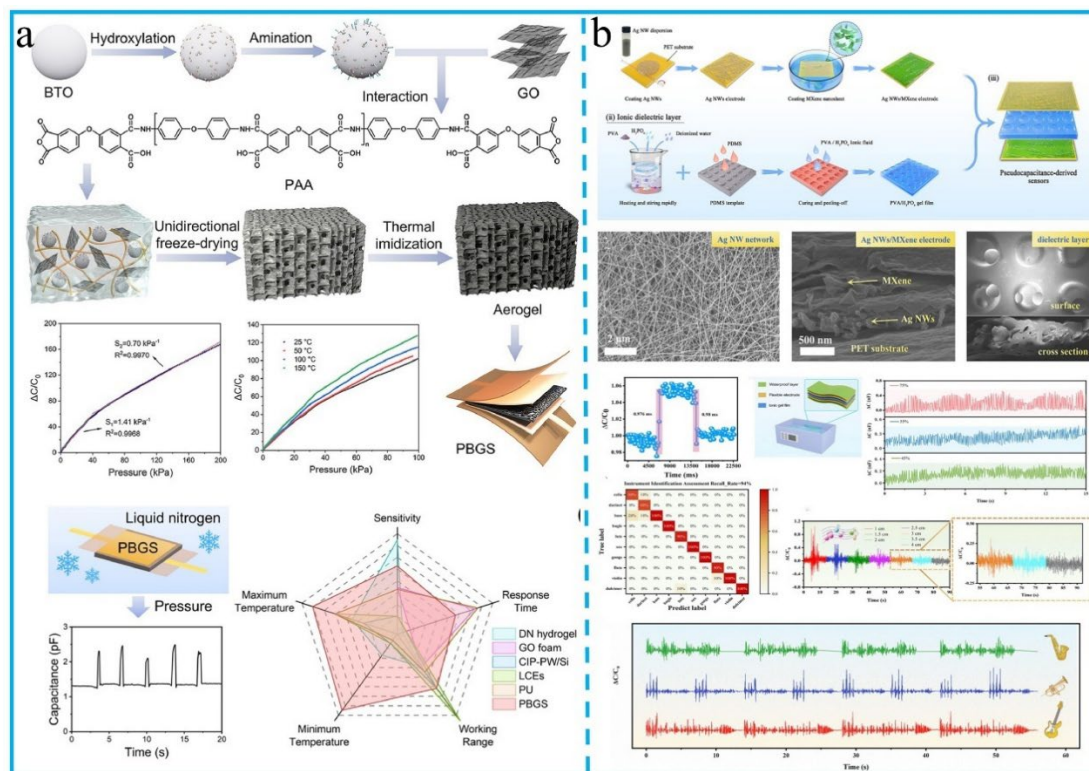


Figure 5. (a) The fabrication process of PI/BTO/GO aerogels and its capacitive sensing and mechanical performance [78]. Copyright 2025, Elsevier. (b) Relative capacitance variation. (b) The preparation process of iontronic capacitive sensor and its sensing performance [79]. Copyright 2024, Elsevier.

To address the aforementioned issues, researchers have carried out a series of endeavors [80]. In terms of materials, efforts have been directed toward developing new dielectric materials with intrinsic compositions and microstructures to enhance their stability, dielectric constant, and mechanical properties, thereby increasing sensing performances and reducing the impact of environmental factors such as temperature on capacitance values [80,81]. For instance, polymer materials with special molecular structures are adopted, whose dielectric properties remain stable over a wide temperature range. In structural design, the structure of capacitive sensing units is optimized by employing a differential structure, which effectively minimizes the influence of external interference and parasitic capacitance [82–84].

Cheng et al. used polyimide (PI) with excellent heat resistance as the substrate, fabricated PI/BTO/GO aerogels via freeze-drying, and assembled them into capacitive sensors (Figure 5a). The oriented aerogel structure and filler interactions enhance mechanical and thermal stability. The sensor operates stably at -196°C to 150°C , maintaining performance over 2000 cycles at 150°C , enabling extreme environment applications. Su et al. develop an iontronic capacitive sensor with Ag NWs/MXene composite electrodes and a $\text{H}_3\text{PO}_4/\text{PVA}$ dielectric layer featuring surface-pillar and internal random multi-bubble structures (Figure 5b). The sensor achieves exceptional linear sensitivity ($\sim 153.83 \text{ kPa}^{-1}$) over 0–260 kPa ($R^2 > 0.996$), rapid response/recovery ($< 1 \text{ ms}$), and stability over 10,000 cycles, functioning underwater. The composite electrode enhances electron conduction and pseudocapacitance, and the dielectric layer design expanding the linear range. It effectively

monitors ultrasonic vibrations, recognizes sound waves and musical instruments, showing great potential in flexible electronics. Moreover, sensing performance and temperature stability of sensors can be achieved via compensation circuit design, MEMS technology, thermal insulation packaging, etc [85–87].

3.5. Piezoresistiv

Piezoresistive vibration sensors operate based on the piezoresistive effect. In 1856, William Thomson (Lord Kelvin) discovered that the resistance of metal materials changes when subjected to mechanical stress, a phenomenon named the piezoresistive effect [88]. Later, it was found that semiconductor materials exhibit a more significant piezoresistive effect, with a good linear relationship between their resistance change rate and the applied stress, enabling more accurate conversion between mechanical and electrical signals [89]. With the advancement of research, semiconductor materials such as single-crystal silicon and germanium, as well as metal strain gauges, have been successively applied in piezoresistive sensors, greatly expanding their performance and application fields. In recent years, the emergence of new piezoelectric material systems based on nano-conductive network reconstruction and tunneling effect, such as polymer/conductive filler composite systems, carbon-based aerogels, and ionic gels, has enabled piezoresistive vibration sensor devices to show great application prospects in fields such as large-amplitude monitoring, environmental stability, biocompatibility, and flexible equipment [90,91].

The structure of a piezoresistive vibration sensor generally includes components such as piezoresistive elements, elastic sensitive elements, mass blocks, a housing, and leads. It boasts advantages such as easy signal processing, simple structure, and low cost. It performs excellently in low-frequency vibration and even quasi-static signal measurement, and is commonly used in scenarios requiring low-frequency vibration monitoring, such as equipment structure vibration monitoring and automobile chassis vibration monitoring [92,93]. The main problems with piezoresistive sensitive materials are as follows: poor temperature stability, where temperature changes can cause zero drift and sensitivity variations, affecting measurement accuracy in environments with large temperature fluctuations; insufficient long-term stability, as their performance will attenuate to a certain extent with prolonged use; nonlinear response under large strains; and relatively high power consumption, requiring external power supply for operation [94]. To address these issues, researchers propose to integrate temperature compensation circuits, adopt materials with low temperature coefficients, optimize packaging to reduce environmental erosion, develop piezoresistive materials, and integrate energy-harvesting modules, aiming to enhance measurement accuracy, durability, and energy efficiency. Among them, heterogeneous composite and microstructure design have become the main breakthrough directions in the design and construction of piezoresistive materials [95].

As shown in Figure 6a, Yan et al. uniformly dispersed multi-walled carbon nanotubes in polydimethylsiloxane (PDMS) to construct a “conductive-elastic” substrate. A hierarchical porous structure was prepared by a sacrificial template method, and a pyramid array was constructed on the surface of the composite membrane. This design utilizes the stress concentration at the tip of the pyramid to enhance sensitivity and relies on the compressive deformation of the porous structure to broaden the pressure detection range. The pressure sensing range of the sensor is 1 Pa-1000 kPa, with a sensitivity of 0.71 kPa⁻¹ in the range of 1-80 kPa and 0.024 kPa⁻¹ maintained at 80-1000 kPa. In addition, it can detect dynamic mechanical stimuli exceeding 20 kHz with a frequency resolution of 0.1 Hz. The electrodes are seamlessly connected to the sensor through chemical bonding, and thus the response-relaxation time is only 0.04 ms.

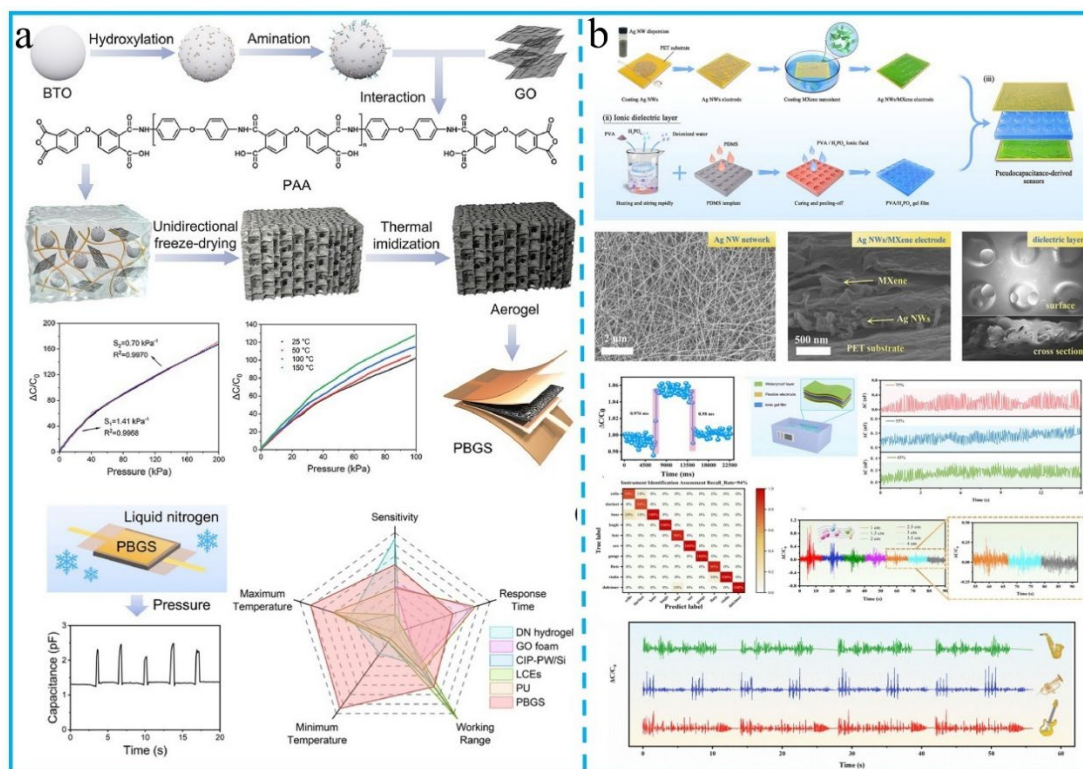


Figure 6. (a) Piezoresistive flexible pressure sensor by combining porous materials with a pyramid array composite hierarchical structure. Reproduced with permission [96]. Copyright 2025, Elsevier. (b) Schematic preparation of biomass-derived aerogel and its strain and vibration sensibility [97]. Reproduced with permission. Copyright 2025, John Wiley and Sons.

Tan et al. presents a biomass-derived piezoresistive aerogel designed via a multiscale microstructure modulation strategy inspired by wood cell assembly (Figure 6b). The aerogel integrates lignin (rigid segments) and cellulose (flexible segments) into a cross-linked network, with oriented micropores and a polypyrrole conductive network. The prepared sensors exhibited exceptional superelasticity (94.91% stress retention after 500 compression cycles at 50% strain) and outstanding sensing performance: an ultra-low detection limit (4.6 Pa/0.01% strain), high sensitivity (160.93 kPa⁻¹, gauge factor 3364), and fast response (11 ms compression, 38 ms rebound). It effectively monitors subtle motions (pulse, swallowing) and substantial movements (joint activities). Combined with deep learning, it enables 96.33% accurate sign language recognition and wireless robotic control, offering a promising platform for proactive health monitoring and advanced human-computer interaction.

3.6. Triboelectric

Triboelectric vibration sensors achieve the sensing and conversion of vibration signals based on the triboelectric effect [98]. In 2012, Wang Zhonglin's research team first proposed the concept of triboelectric nanogenerators (TENGs), whose core principle relies on the coupling effect of contact electrification and electrostatic induction during the contact-separation process of two different materials [99]. When vibrations cause mechanical contact and separation between the surfaces of triboelectric materials, interfacial charge transfer creates a surface potential difference, generating induced current or voltage signals in the external circuit. This enables the direct conversion of mechanical energy to electrical energy, with the output electrical signals having a clear correlation with vibration parameters such as amplitude and frequency. Subsequently, researchers have developed a diverse range of triboelectric material systems, including positively charged materials (e.g., nylon, cellulose, metal foils), negatively charged materials (e.g., polytetrafluoroethylene (PTFE),

PDMS, PI, and various micro-nano structured modified composites, further expanding their applicability in vibration sensing [100].

The structure of triboelectric vibration sensors typically includes components such as triboelectric material layers, electrode layers, support structures, and signal processing circuits. These sensors exhibit significant advantages including excellent self-powered capability, a wide range of material choices, flexible structural design, low cost, and high sensitivity to low-frequency vibrations [17]. They are widely used in low-frequency vibration monitoring scenarios, such as health monitoring of large structures like bridges and buildings, as well as detection of weak vibration signals from human motion and sound waves. However, affected by material surface charge stability and environmental factors, triboelectric vibration sensors still face challenges in measurement accuracy and environmental adaptability.

Environmental humidity is one of the key factors affecting the performance of triboelectric sensors. High humidity accelerates the dissipation of surface charges on materials, thereby reduce the strength and stability of output signals [101]. To address this issue, researchers have developed techniques such as material surface modification and structural encapsulation [102]. Besides, the triboelectric effect relies on contact-separation on material surfaces, traditionally structured sensors tend to experience incomplete contact or response lag under high-frequency vibrations, leading to decreased measurement accuracy.

Thus, researchers have improved high-frequency response characteristics by optimizing micro-nano structures and adopting new working modes. As shown in Figure 7a, Huang et al. designed a cavity-free membrane TENG. Guided by 3D laser-scanned broadband vibration characteristics of the FEP membrane, it eliminates the cavity, enabling contact electrification independent of ultrasonic excitations. It achieves an ultralow detection limit of 37.1 Pa@20 kHz, average 206.1 Pa (20–200 kHz), 1-2 orders lower than conventional designs. With 0.001 kHz frequency resolution, 25 MHz operating frequency, and stability over 100 million cycles, it performs well in diverse ultrasonic vibration sensing.

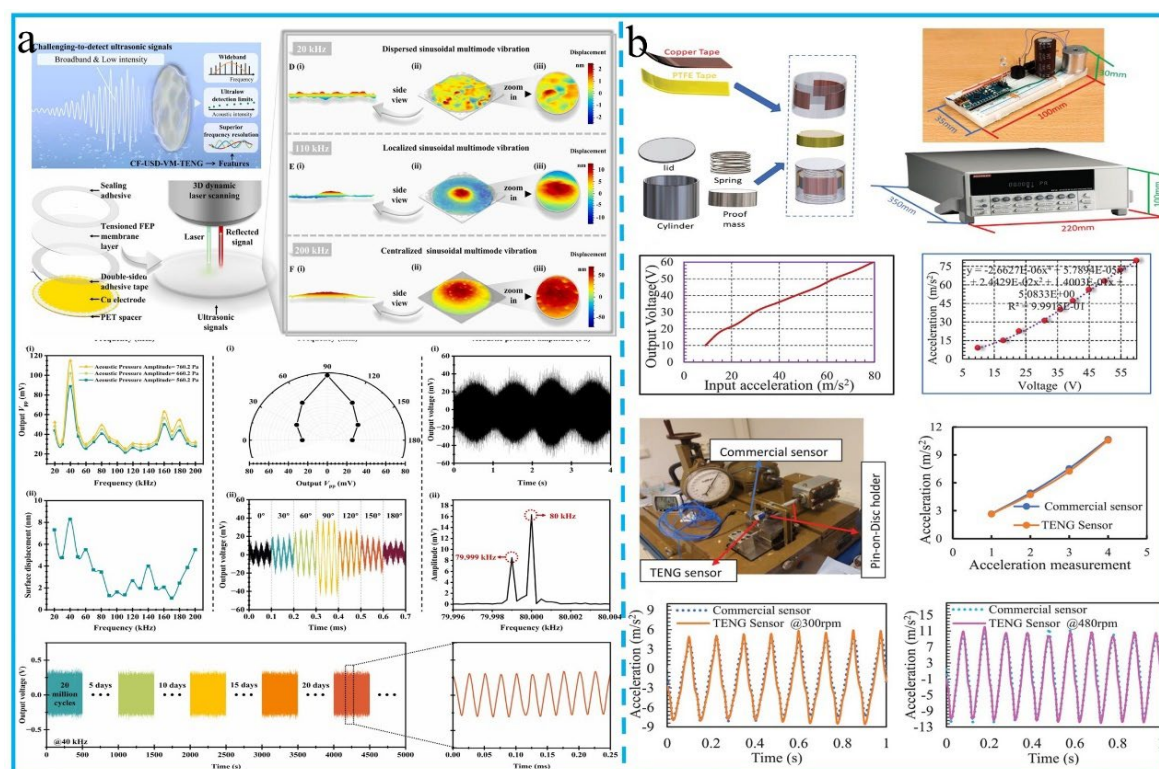


Figure 7. (a) Concept and vibration monitoring performances of cavity-free membrane TENG [103]. Copyright 2025, Elsevier. (b) Structure and materials design of the miniaturized TENG-based vibration sensing device and its acceleration sensing performance [104]. Copyright 2023, John Wiley and Sons.

vibration wireless sensing system and its application on the vehicle engine monitoring [110]. Reproduced with permission. Copyright 2025, Elsevier. (c) MXene/CNF aerogel@PDMS-based dual-modal pressure sensor and its multiple sensibility [111]. Reproduced with permission.

4. Application of Vibration Sensors on Industrial Monitoring

In modern industry, equipment reliability and safety are crucial for ensuring production efficiency. Faults in critical moving components, performance degradation caused by structural damage, and frictional failures resulting from lubrication degradation all manifest through characteristic changes in vibration signals [14]. Moreover, vibration monitoring can be used for early fault prediction and remaining life assessment, propelling the industrial maintenance from post-failure repair to predictive service [19]. As a cross-disciplinary solution integrating sensing technology, signal processing, structural dynamics, and intelligent algorithms, currently, vibration sensors are developing towards wide-frequency monitoring, high precision, self-powered operation, and high environmental stability, aiming to construct a technological cornerstone for ensuring equipment reliability in the era of IoT, AI, and intelligent manufacturing [11].

4.1. Fault Diagnosis

Motion joints such as bearings and gears serve as core components for power transmission, whose operational reliability directly impacts equipment efficiency and safety. Typical faults, including bearing damage, gear wear, and shaft unbalance, can induce changes in system dynamic characteristics, thereby generating vibration responses with deterministic patterns [112]. For example, bearing fault frequencies are directly related to the number of rolling elements, geometric dimensions, and rotational frequency and are centered around high-frequency impacts and characteristic frequencies; gear fault frequencies are closely related to the meshing frequency and are marked by modulation sidebands and higher amplitude [29].

Sensors should be deployed near monitored vibration component, such as bearing housings or gearbox casings, to obtain raw signals with the optimal SNR. Subsequently, fault features are determined through signal processing techniques. For example, frequency-domain analysis based on the Fourier transform is suitable for extracting fault characteristic frequencies, while time-frequency methods like the Short-Time Fourier Transform can effectively capture transient fault features during start-up/shut-down processes; for variable-speed equipment, signal processing techniques such as order analysis eliminate the interference of rotational speed fluctuations on fault feature extraction [14]. Finally, by comparing and analyzing vibration spectra with those in healthy states, quantitative identification of abnormal frequency components is achieved. In recent years, the development of multi-sensor fusion technology, deep learning, and other technologies has driven fault diagnosis to evolve from traditional signal processing to multi-dimensional and intelligent diagnosis, providing new technical pathways for intelligent operation and maintenance of industrial equipment [113].

Sensor performance is crucial for achieving accurate monitoring. Its monitoring range must comprehensively cover equipment operating conditions and fault characteristic parameters. For example, high-frequency impacts can reach over 20 kHz, which is suitable for using a piezoelectric sensor; the amplitude deviation of high-precision bearings is extremely small, and thus capacitive sensing might be more appropriate [114]. Facing complex industrial environments, sensors need to have strong environmental robustness (temperature, humidity, electromagnetic, etc.). Besides, to ensure the accuracy of signal analysis, parameters such as resolution and measurement error are critical.

Huang et al. developed the multilongitudinal mode quadrature laser self-mixing vibration sensor [60]. Leveraging the spacing characteristics of multilongitudinal mode lasers, they generate two polarized self-mixing signals with tunable phase shifts and then measure target vibrations through relevant quadrature demodulation techniques, quadrature-phase algorithm, and circle fitting. Demonstrated in bearing fault diagnosis, the sensor achieved 5.00 μm amplitude measurement error less than 40 nm and bearing frequency error less than 0.65%. Its high accuracy,

compactness, and robustness promise wide applications in online measurement and dynamic analysis.

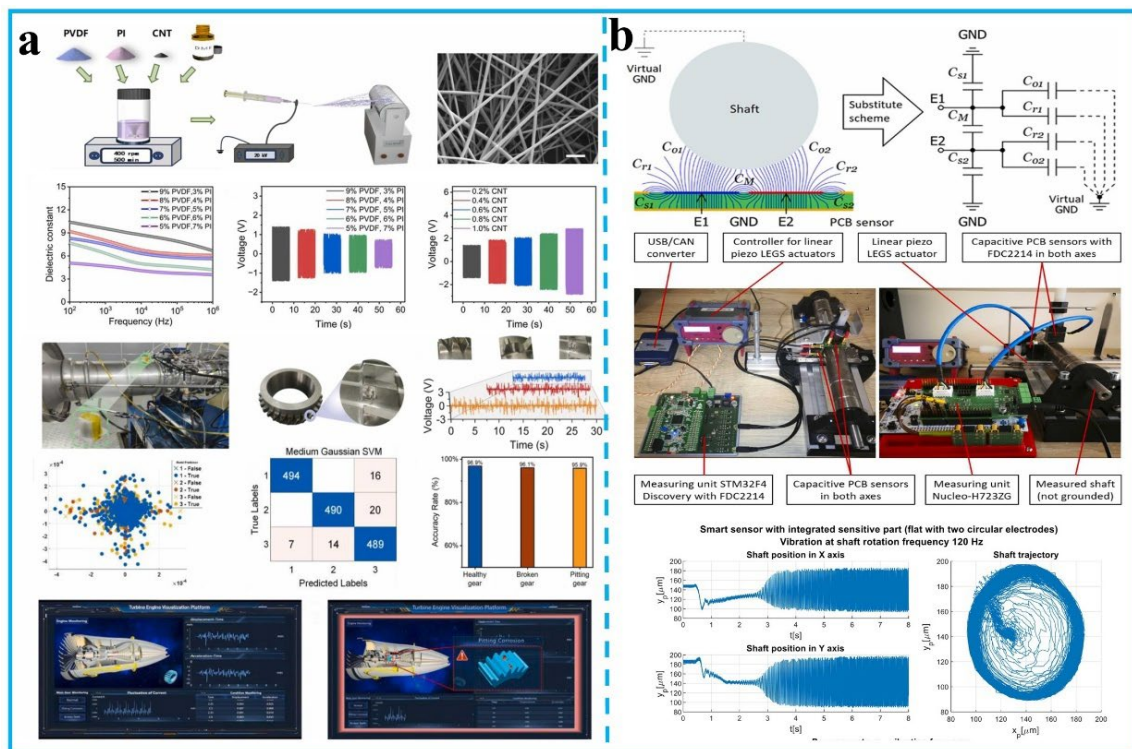


Figure 9. (a) Manufacturing, morphology, and output voltage of the composite membrane and its application in gear faults recognition and digital twin demonstration [115]. Reproduced with permission. Copyright 2025, Elsevier. (b) The principle measuring mechanism of the designed capacitive vibration sensor and its deployment on a high-speed laboratory machine monitoring [116]. Reproduced with permission. Copyright 2024, Elsevier.

As shown in Figure 9a, Hu et al. presents a self-powered piezoelectric vibration sensor, with a layered structure of tungsten, polyethylene terephthalate, aluminum, and the PVDF-PI nanofiber membrane [115]. The synergistic designed sensor can distinguish vibration signals from healthy, pitting, and broken gears with a 96.3% recognition accuracy using machine-learning algorithms. Due to the thermal stability of PI and enhancement of carbon nanotubes, the sensor maintains stable electrical output under high temperatures (e.g., only 15% performance decline at 80°C). Furthermore, a digital twin system is developed to integrate physical sensor data, information processing, and virtual modeling for real-time fault diagnosis and engine health management. Pawlenka et al. develops custom capacitive sensors for measuring vibrations and small displacements in high-speed rotating machines (Figure 9b). The sensors exhibited a maximum measurement frequency of 3.8 kHz, a maximum relative error of about 0.7%, and a resolution ranging from 700 nm to 14 μm . Smart sensors with integrated sensitive parts show optimal performance, verifying their suitability for shaft displacement diagnosis and active vibration control.

In addition, problems in the control system can also cause characteristic signals in the vibration of the transmission system, and thus fault reporting can be achieved through vibration signal analysis. Papathanasopoulos et al. propose a non-invasive technique for fault diagnosis of position control system in brushless DC motor drives, leveraging vibration signals acquired by low-cost piezoelectric sensors [117]. As position control system faults (i.e., misalignment or breakdown), characteristic signal manifest in vibration signatures, where the second harmonic component serves as a reliable signature for misalignment faults, and the fourth harmonic component is used to detect breakdown faults.

4.2. Structural Health Monitoring

The equipment structural health monitoring (SHM) technology based on vibration sensing is an interdisciplinary field integrating sensing technology, structural dynamics, signal processing, and recently, machine learning [118]. Its core theory posits that structural damages, such as cracks, fatigue, and loosening, alter the stiffness, damping characteristics, and other mechanical properties of the vibration system. Consequently, these changes affect the intrinsic vibration parameters of structural components, including NF and modal shapes [119]. For instance, crack propagation reduces local stiffness, shifting the structural NF to the low-frequency range; while the loosening of connected components introduces nonlinear stiffness, resulting in subharmonic vibration.

In practical engineering monitoring, vibration sensors are attached to or embedded within structural surfaces or interiors to convert structural vibration induced into electrical or optical signals. Collected signals, typically containing complex environmental noise and nonlinear components, are processed and analyzed to determine current inherent vibration parameters, such as the NFs, damping ratios, and mode shapes. These real-time parameters are assessed with baseline data, which is established under healthy structural conditions. Then, damage is identified when the deviation from the baseline reaches a predefined threshold [120].

At present, piezoelectric sensors dominate the traditional SHM market, but they have problems such as poor low-frequency response and being vulnerable to electromagnetic interference. Fiber optic sensors have strong anti-interference ability and good durability, but their dynamic response bandwidth is limited (usually < 1 kHz), which is insufficient for the monitoring of high-speed equipment. MEMS accelerometers have advantages such as low cost and miniaturization, but the noise level limits their high-precision applications. Along with technical challenges such as power supply and signal transmission, SHM vibration sensors develop towards directions of power-free, wireless transmission, and functional integration [121].

For example, Cui et al. proposed a disk-shaped TENG, which uses multi-sized honeycomb structures and PTFE balls as friction materials (Figure 10a). It can achieve broadband vibration detection from 10-2000 Hz, with an acceleration measurement range of 1-11 m/s^2 and a resolution of 0.1 m/s^2 . Under the vibration condition of 11 m/s^2 , the peak voltage exceeds 80 V, and it can charge a 100 pF capacitor to 5 V within 100 seconds. Subsequently, with a dedicated circuit, it was used for wireless self-powered vibration detection, demonstrating its feasibility for the structural health monitoring of motors, tracks, etc.

Besides, with the continuous advancement of MEMS and wireless sensing technologies, and the application of flexible sensor arrays, novel approaches have emerged for the distributed real-time monitoring of complex curved structures, such as aero-engine blades and wind turbine blades. In the field of intelligent diagnosis, machine learning algorithms, trained on extensive labeled vibration datasets, enable accurate identification of structural damage patterns, locations, and severity levels [122–124].

As shown in Figure 10b, Muxica et al. prepared an autonomous on-blade sensor system for remote vibration measurement of low-capacity wind turbine blades. Deployed on three turbines, including one in harsh southern Chile, the system uses MEMS accelerometers to record flapwise/edgewise accelerations, enabling dynamic characteristic extraction for structural damage diagnosis. Powered by solar panels and Li-ion batteries, it achieves reliable data acquisition/transmission without human intervention. The system demonstrates 99.6% data transmission reliability and accurately captures NFs, laying a foundation for vibration-based structural health monitoring. Its cost-effective, autonomous design withstands extreme environments, showcasing potential for long-term blade health evaluation.

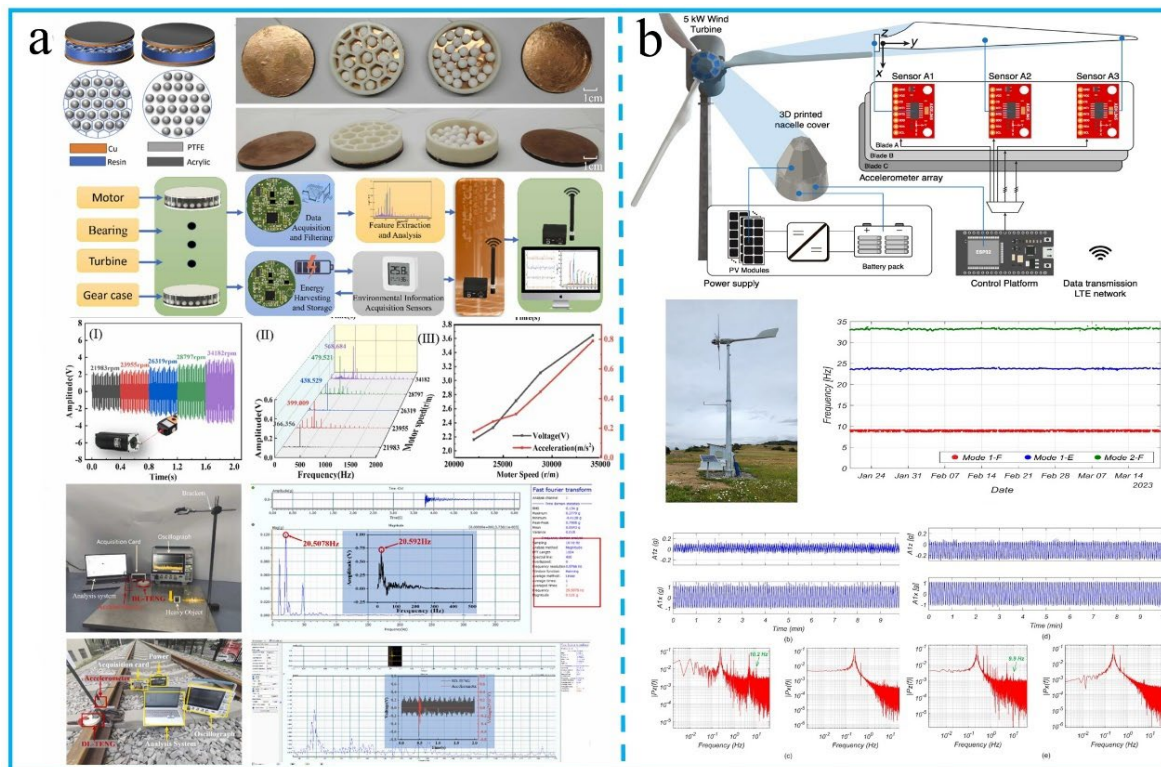


Figure 10. (a) Structure of the TENG and as-assembled vibration sensor and its application for structure monitoring of motor and railroad tracks. Reproduced with permission [125]. Copyright 2025, Elsevier. (b) Overview of the embedded detection system for wind turbine blades and vibration measurement signals. Reproduced with permission [126]. Copyright 2025, MDPI.

4.3. Tribological Status Analysis

The degradation of equipment lubrication status essentially represents imbalanced physicochemical interactions on the friction surfaces. Insufficient lubrication leads to increased energy loss and wear of critical frictional components, thereby reducing the operational efficiency and service life of equipment. In cases of poor lubrication, the friction coefficient at the frictional contact interface rises sharply. According to Coulomb's law of friction, the rapidly increased friction-induced contact stress generates high-frequency mechanical impacts via micro-elastic-plastic deformation, which in turn excite wide-frequency random vibrations. The interaction between tribological conditions and vibrational behaviors is the basis for monitoring lubrication status using vibrations [127,128]. Furthermore, friction-induced vibrations can increase the risk of mechanical structures damage and affect the machining accuracy of products [129]. Therefore, monitoring lubrication status through vibration analysis is of great significance for improving both the service life and production efficiency of equipment [130].

Variations in frictional operating conditions, such as frictional motion behaviors (sliding friction, rolling friction, fretting friction), lubrication states (fluid lubrication, mixed lubrication, boundary lubrication, dry friction, etc.), and the wear condition, can induce changes in contact behaviors, friction coefficients, and energy dissipation mechanisms between friction pairs, thereby generating corresponding characteristic vibration signal spectrums [131–134]. Based on these vibration characteristics, it is necessary to select appropriate vibration sensors for effective monitoring, so as to ensure that the sampling accuracy meets the requirements of subsequent analysis. For instance, piezoelectric sensors are suitable for capturing high-frequency vibrations from abnormal gear meshing and local bearing defects. Capacitive/inductive displacement sensors, meanwhile, can dynamically measure the oil film thickness of low-speed heavy-load equipment with a measurement accuracy reaching the sub-micron level.

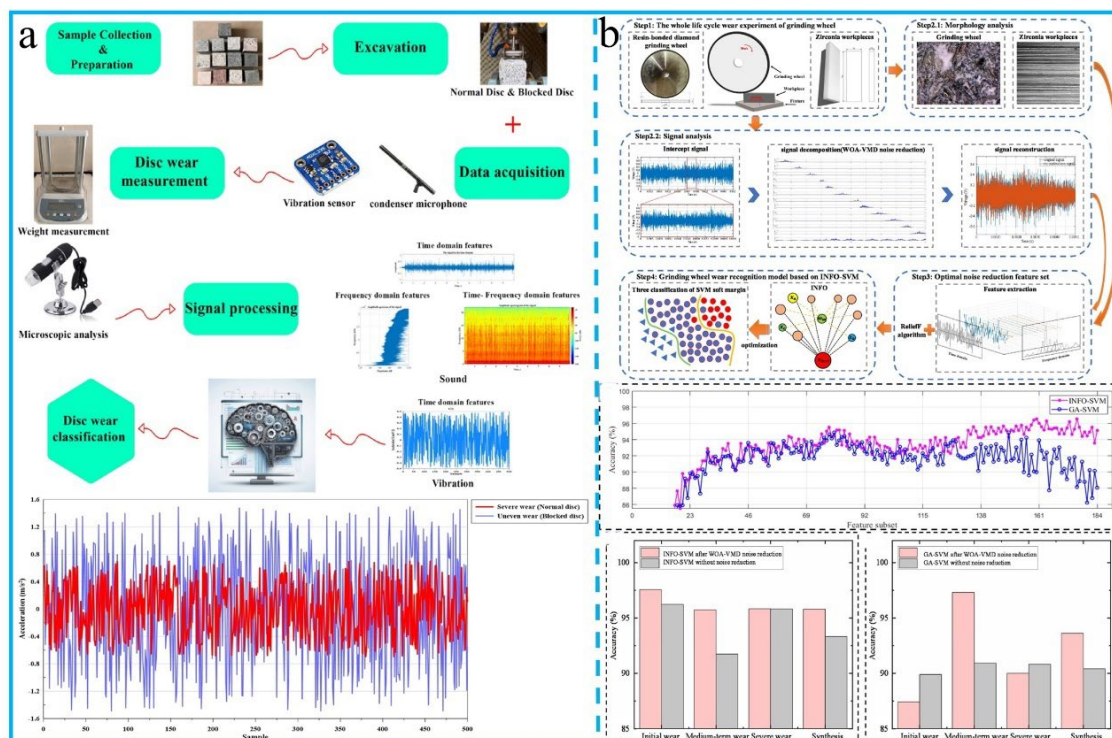


Figure 11. (a) The framework of the proposed sound and vibration sensor-based approach with machine learning technique and its application in wear identification [135]. Copyright 2024, Elsevier (b) Grinding wheel wear status recognition architecture based on optimized modal and its identification accuracy of feature subset [136]. Copyright 2025, Elsevier.

Signal analysis technology is also a core component of lubrication condition diagnosis. On the one hand, researchers explore the generation mechanism and physical essence of vibration signals through the research of lubrication-vibration coupling dynamics, etc., and then establish the characteristic frequency generation mechanisms [137,138]. On the other hand, by means of various signal analysis methods, including traditional methods such as time-domain analysis and adaptive decomposition, as well as new data processing technologies such as deep learning, the characteristic frequencies of the lubrication state are identified [11,139]. Research on vibration sensor devices in the field of lubrication state monitoring has formed a full-chain technical system from basic theory to engineering application. However, it still faces many challenges such as sensitivity, accuracy, and environmental adaptability. Therefore, researchers try to make improvements through methods such as new sensing mechanisms, miniaturization, intelligentization, and fusion diagnosis to meet the increasing requirements on industrial equipment lubrication monitoring [140].

As shown in Figure 11a, Bagherpour et al. integrated sound and vibration sensing with machine learning techniques to achieve real-time monitoring for disc cutter wear in tunnel boring machines. The research reveals that sound and vibration signals correlate significantly with wear progression, particularly in the frequency range of 3.5-8 kHz for normal wear and 3.5-13 kHz for blocked cutters. This approach enables non-intrusive, continuous wear assessment without disrupting excavation and offer a practical solution for real-time tool wear evaluation, guiding optimal replacement timing and enhancing safety in underground construction. Wan et al. present a multi-sensor monitoring methodology for grinding wheel wear evaluation (Figure 11b). It combines Whale Optimization Algorithm and Variational Mode Decomposition for signal denoising, which distinguishes grinding process and environmental noise frequency bands, enhancing SNR by 30% compared to other methods. Using the Relieff algorithm for feature selection, it constructs a dataset and develops a model that optimizes Support Vector Machine parameters via the weighted mean of vectors algorithm. Innovatively, it integrates image analysis of grinding wheel and workpiece with multi-sensor signals (AE, force, vibration). The optimized model achieves 95.8% accuracy with

a fast recognition time of 1.1769s, showing superior robustness and efficiency in handling low-correlation datasets, outperforming traditional methods. This integration of direct observation and indirect monitoring advances wear evaluation precision.

4.4. Early Warning and Service Life Prediction

Vibration sensors can realize early fault warning and remaining useful life (RUL) prediction via acquiring mechanical vibration signals in real time, analyzing characteristic parameters, and integrating intelligent algorithms. Its core lies in quantifying the degradation process of equipment health status, combining the physics of failure model with data-driven methods, and establishing the relationship among vibration characteristics, damage accumulation, and life consumption [141]. After convert mechanical vibration into electrical signals, the data undergo multistage processing procedures including filtering, amplification, and feature extraction. For example, the Fast Fourier Transform is employed to convert time-domain signals into the frequency domain for identifying fault characteristic frequencies, and envelope analysis technique is combined to demodulate high-frequency signals, further highlighting early fault features [142,143]. Then, the characteristic vibration signal thresholds are set to construct a hierarchical early warning system. By continuously tracking feature trends (e.g., RMS values and high-frequency energy), time-series curves of equipment operation status are generated to realize life prediction. For example, Thoppil et al. combined principal component analysis and exponential degradation model for mechanical system RUL prediction [144]. By extracting time-frequency features with discrete wavelet transformation and selecting them via monotonicity, trendability and prognosability, Health Indicator was successfully established to estimate RUL. Validated on FEMTO bearing data, the HI effectively reflects degradation, with RUL prediction error at 21 minutes, showing potential for predictive maintenance.

In recent years, the introduction of artificial intelligence models has significantly improved prediction accuracy [145,146]. For instance, the Long Short-Term Memory network learns historical vibration data sequences to predict the degradation trajectory of equipment within 7–30 days, while the Convolutional Neural Network identifies abnormal patterns in vibration spectrograms for early fault warning. Combined with probabilistic models like Weibull distribution and survival analysis, these models quantify the RUL of equipment. Moreover, intelligent analysis based on vibration monitoring data enables comprehensive optimization of maintenance strategies. On one hand, the early warning system automatically generates predictive work orders, planning maintenance schedules and spare parts orders in advance to reduce unplanned downtime. On the other hand, equipment operation parameters can be optimized according to vibration data, achieving energy efficiency improvement and RUL extension.

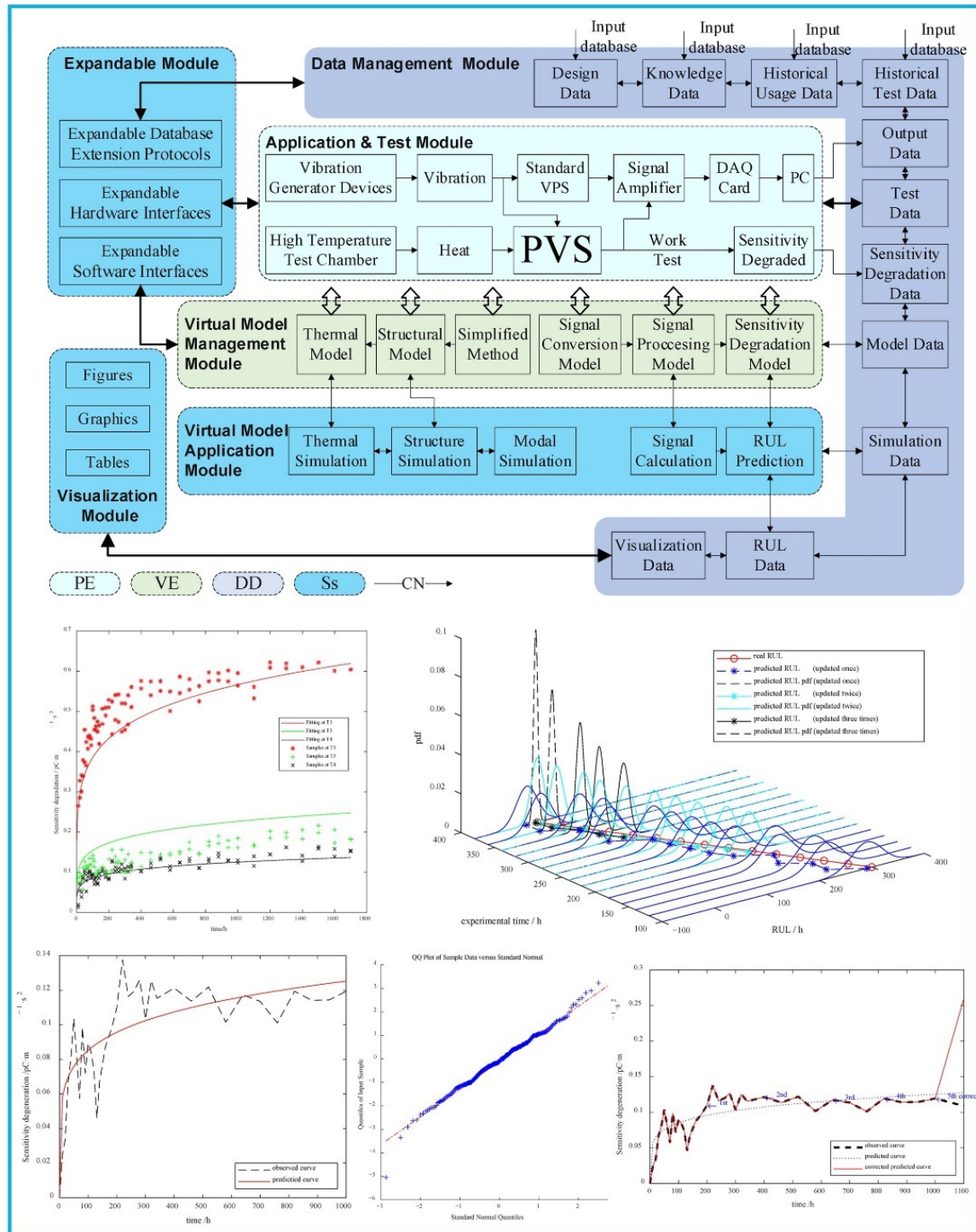


Figure 12. A digital-twin framework for predicting RUL with sensitivity degradation modeling [147]. Copyright 2023, MPDI.

Current RUL prediction is still confronted with several core issues: poor adaptability to working condition transitions, where the mapping between vibration and service life of the same equipment drifts under varying loads, leading to a high prediction error; insufficient quantification of uncertainty, which fails to effectively characterize the randomness of the degradation process and thus results in an excessively wide RUL prediction uncertainty; and the contradiction between high sampling frequency and low power consumption. To tackle these problems, researchers have proposed solutions including intelligent model evolution and autonomous decision support [148]. For example, Fu et al. establishes a digital-twin framework based on a five-dimensional predicted model,

integrating six modules for sensitivity degradation detection (Figure 12). The framework employs a Wiener-Arrhenius accelerated degradation model to characterize temperature-induced sensitivity degradation, coupled with real-time error correction via the Akaike information criterion and Bayesian parameter updating. Experiments on PVS samples demonstrate that the model reduces prediction errors to 8 hours.

5. Conclusion and Future Prospects

Vibration sensors, serving as core sensing components in industrial systems, are essential for monitoring equipment structural health and assessing operational status. Leveraging physical principles such as the piezoelectric effect and piezoresistive effect, these sensors utilize sensitive materials to convert mechanical vibration signals into electrical signals, enabling precise measurement of key parameters like vibration frequency, acceleration, and displacement. Recent advancements in materials science and micro/nano-fabrication technologies have propelled significant progress in vibration sensor technology.

The development of novel sensitive materials, adoption of advanced manufacturing processes, and exploration of innovative sensing mechanisms have driven sensor performance towards higher precision, miniaturization, wearability, and self-power generation capabilities [149–153]. These evolutions mark a technological leap from traditional electromechanical sensors to intelligent microsystems. Looking forward, the future development of vibration sensors will focus on new material development, advanced manufacturing innovation, multi-sensor integration, miniaturization, and intelligentization, all aimed at meeting the urgent needs of predictive maintenance and system optimization in intelligent manufacturing. These developments will significantly reduce equipment failure rates and maintenance costs, and exhibit broad application prospects in fields such as industry, transportation, and aerospace.

New materials: Intergrating emerging material systems, including nanomaterials, green materials, and smart materials, significantly enhances the overall performance of vibration sensors. Nanomaterials such as graphene and carbon nanotubes, with their outstanding physicochemical properties, mechanical strength, and electrical characteristics, can boost device sensitivity and improve adaptability in extreme environments (e.g., high temperature, radiation, corrosion), meeting the long-term monitoring demands for aerospace and nuclear equipment [154,155]. Advanced biodegradable materials, such as cellulose nanocrystal/polylactic acid composites, match the performance of conventional plastics while substantially reducing electronic waste pollution [156,157]. Self-healing polymers endow sensing device with self-repairing functions, enabling the device to recover after severe damage [158]. TENG materials smartly achieve the utilization of vibration energy and self-powered monitoring of vibration signals through delicate design [125].

New manufacturing technologies: Breakthroughs in novel manufacturing technologies, including controlled composite processes, surface microstructural engineering, and additive manufacturing, are reshaping the vibration sensor development. Controlled composite technologies overcome the performance trade-offs of conventional composite material, enabling synergistic optimization of multi-capacities [159,160]. Surface microstructural engineering innovations (e.g., infrared thermal shaping, UV-pulsed cold processing, light-induced surface reconstruction) achieve precise microstructural control over shape-memory alloys, hydrogels, and liquid metals to improve micro-vibration detectability [161]. Additive manufacturing techniques leverage flexible multi-dimensional structuring to fabricate integrated anisotropic sensing units [162,163]. These advances drive transformative innovations in material systems and structural designs, accelerating the sensor transition to high performance and miniaturization.

Multi-sensor fusion strategy: Multi-sensor fusion technology relies on two core strategies to achieve precise perception and evaluation of the vibration systems. Heterogeneous sensor fusion modal integrates data from vibration sensors with different measurement principles (e.g., piezoelectric acceleration sensors, electromagnetic velocity sensors, and capacitance displacement sensors), overcoming single-sensor measurement limitations and enabling multi-perspective

reconstruction of the measured object's vibration characteristics [109]. Cross-domain sensor fusion modal jointly processes multi-source data (e.g., acceleration, strain, temperature) reflecting equipment operating states [159,164]. This strategy can construct a multi-dimensional feature space that significantly improves the monitoring data accuracy and reliability, and endows the system with adaptive robust characteristics.

Miniaturization and intelligentization: With the development of miniaturization technologies, such as MEMS, sensors and signal processing circuits can be integrated into tiny chips, featuring small size, light weight, power efficiency, mass production, and low costs [165]. They show great application potential in space-constrained fields like aerospace and biomedicine, providing innovative solutions for precision equipment monitoring and disease diagnosis and treatment [166,167]. Intelligent sensors, by integrating sensors with smart chips, can perform real-time processing on collected vibration signals, including signal transform, feature extraction, data comparison, and even performance prediction [168,169].

Author Contributions: Conceptualization, writing—original draft preparation, M.M; writing—review and editing, Z.L. and J.W.; supervision, S.Y. and J.W. All authors have read and agreed to the published version of the manuscript.

Funding: This work was supported by the Strategic Priority Research Program of the Chinese Academy of Science (No. XDB 0470301), the National Natural Science Foundation of China (No. 52175203 and 52375218), and Major Science and Technology Project of Gansu Province (No. 23ZDGA011).

Conflicts of Interest: The authors declare no conflicts of interest.

Abbreviations

The following abbreviations are used in this manuscript:

SNR	signal-to-noise ratios
E	total energy
A	amplitude
k	elastic coefficient of the system
NF	natural frequency
m	mass of the block
E_k	kinetic energy
E_p	potential energy
RMS	root mean square
x	displacement of the mass block
a_{max}	acceleration amplitude
ω	angular frequency
MAPE	mean absolute percentage error
R^2	coefficient of determination
PZT	lead zirconate titanate
BTO	barium titanate
PVDF	polyvinylidene fluoride
T_c	Curie temperature
MEMS	Micro-Electro-Mechanical Systems
GO	graphene oxide
PI	polyimide
PVA	polyvinyl alcohol
NWs	nanowires
PDMS	polydimethylsiloxane
TENG	triboelectric nanogenerator
PTFE	polytetrafluoroethylene
CNF	carbon nano fiber
DC	direct current
SHM	structural health monitoring

RUL remaining useful life

References

- Harms, J.; Ambrosino, F.; Angelini, L.; Braitto, V.; Branchesi, M.; Brocato, E.; Cappellaro, E.; Coccia, E.; Coughlin, M.; Della Ceca, R.; et al. Lunar Gravitational-wave Antenna. *Astrophys. J.* **2021**, *910*, 1, <https://doi.org/10.3847/1538-4357/abe5a7>.
- Maresca, R.; Guerriero, L.; Ruzza, G.; Mascellaro, N.; Guadagno, F.M.; Revellino, P. Monitoring ambient vibrations in an active landslide: Insights into seasonal material consolidation and resonance directivity. *J. Appl. Geophys.* **2022**, *203*, <https://doi.org/10.1016/j.jappgeo.2022.104705>.
- Velez, S.T.; Seibold, K.; Kipfer, N.; Anderson, M.D.; Sudhir, V.; Galland, C. Preparation and Decay of a Single Quantum of Vibration at Ambient Conditions. *Phys. Rev. X* **2019**, *9*, 041007, <https://doi.org/10.1103/physrevx.9.041007>.
- Mayyas, M. Modeling and analysis of vibratory feeder system based on robust stick-slip motion. *J. Vib. Control.* **2021**, *28*, 2301–2309, <https://doi.org/10.1177/10775463211009633>.
- Chen, Y.; Pan, L.; Yin, Z.; Wu, Y. Effects of ultrasonic vibration-assisted machining methods on the surface polishing of silicon carbide. *J. Mater. Sci.* **2024**, *59*, 7700–7715, <https://doi.org/10.1007/s10853-024-09661-x>.
- Duan, C.; Yuan, J.; Pan, M.; Huang, T.; Jiang, H.; Zhao, Y.; Qiao, J.; Wang, W.; Yu, S.; Lu, J. Variable elliptical vibrating screen: Particles kinematics and industrial application. *Int. J. Min. Sci. Technol.* **2021**, *31*, 1013–1022, <https://doi.org/10.1016/j.ijmst.2021.07.006>.
- Chen, L.; Zeng, Z.; Zhang, D.; Wang, J. Vibration Properties of Dual-Rotor Systems under Base Excitation, Mass Unbalance and Gravity. *Appl. Sci.* **2022**, *12*, 960, <https://doi.org/10.3390/app12030960>.
- Wang, L.; Hu, L.; Zhang, J.; Liao, J. Vibration characteristics of a high-speed turbocharger rotor with mass unbalance based on simulation and experiment. *Proc. Inst. Mech. Eng. Part C: J. Mech. Eng. Sci.* **2024**, *239*, 1607–1623, <https://doi.org/10.1177/09544062241290972>.
- Li, X.; Xu, Y.; Liu, J.; Zhang, Y.; Liu, J.; Pan, G.; Shi, Z. Vibration analysis of the propulsion shaft system considering dynamic misalignment in the outer ring. *J. Sound Vib.* **2024**, *589*, <https://doi.org/10.1016/j.jsv.2024.118612>.
- Li, Y.; Long, T.; Luo, Z.; Wen, C.; Zhu, Z.; Jin, L.; Li, B. Numerical and experimental investigations on dynamic behaviors of a bolted joint rotor system with pedestal looseness. *J. Sound Vib.* **2023**, *571*, <https://doi.org/10.1016/j.jsv.2023.118036>.
- Ghazali, M.H.M.; Rahiman, W.; Tang, G. Vibration Analysis for Machine Monitoring and Diagnosis: A Systematic Review. *Shock. Vib.* **2021**, *2021*, <https://doi.org/10.1155/2021/9469318>.
- Walter, P.L. Review: Fifty Years Plus of Accelerometer History for Shock and Vibration (1940–1996). *Shock. Vib.* **1999**, *6*, 197–207, <https://doi.org/10.1155/1999/281718>.
- P, M.W. Piezoelectricity, its history and applications. *The journal of the Acoustical Society of America* **1981**, *70*, 1561–1566.
- Hassan, I.U.; Panduru, K.; Walsh, J. An In-Depth Study of Vibration Sensors for Condition Monitoring. *Sensors* **2024**, *24*, 740, <https://doi.org/10.3390/s24030740>.
- Hassan, I.U.; Panduru, K.; Walsh, J. Non-destructive testing methods for condition monitoring: A review of techniques and tools. *Procedia Comput. Sci.* **2025**, *257*, 420–427, <https://doi.org/10.1016/j.procs.2025.03.055>.
- Babatain, W.; Bhattacharjee, S.; Hussain, A.M.; Hussain, M.M. Acceleration Sensors: Sensing Mechanisms, Emerging Fabrication Strategies, Materials, and Applications. *ACS Appl. Electron. Mater.* **2021**, *3*, 504–531, <https://doi.org/10.1021/acsaelm.0c00746>.
- Haroun, A.; Tarek, M.; Mosleh, M.; Ismail, F. Recent Progress on Triboelectric Nanogenerators for Vibration Energy Harvesting and Vibration Sensing. *Nanomaterials* **2022**, *12*, 2960, <https://doi.org/10.3390/nano12172960>.
- Burdzik, R.; Khan, D. An overview of the current state of knowledge and technology on techniques and procedures for signal processing, analysis, and accurate inference for transportation noise and vibration. *Measurement* **2025**, *252*, <https://doi.org/10.1016/j.measurement.2025.117314>.
- Hassan, I.; Panduru, K.; Walsh, J. Predictive maintenance in industry 4.0: A review of data processing methods. *Procedia Computer Science* **2025**, *257*, 896–903.

20. Soomro, A.A.; Muhammad, M.B.; Mokhtar, A.A.; Saad, M.H.M.; Lashari, N.; Hussain, M.; Sarwar, U.; Palli, A.S. Insights into modern machine learning approaches for bearing fault classification: A systematic literature review. *Results Eng.* **2024**, *23*, <https://doi.org/10.1016/j.rineng.2024.102700>.
21. Xu, S.; Xing, F.; Wang, R.; Li, W.; Wang, Y.; Wang, X. Vibration sensor for the health monitoring of the large rotating machinery: review and outlook. *Sens. Rev.* **2018**, *38*, 44–64, <https://doi.org/10.1108/sr-03-2017-0049>.
22. Shi, B.; Yang, J.; Wang, J. Forced vibration analysis of multi-degree-of-freedom nonlinear systems with the extended Galerkin method. *Mech. Adv. Mater. Struct.* **2022**, *30*, 794–802, <https://doi.org/10.1080/15376494.2021.2023922>.
23. Peng, H.; Zhang, H.; Fan, Y.; Shanguan, L.; Yang, Y. A Review of Research on Wind Turbine Bearings' Failure Analysis and Fault Diagnosis. *Lubricants* **2022**, *11*, 14, <https://doi.org/10.3390/lubricants11010014>.
24. Zheng, J.; Hu, S.; Ji, J.; Zhang, X.; Tong, V.-C.; Yin, S.; Feng, K.; Dong, H.; Xu, L. A review of fatigue failure and structural design of main bearings in tunnel boring machines based on engineering practical examples. *Eng. Fail. Anal.* **2024**, *163*, <https://doi.org/10.1016/j.engfailanal.2024.108611>.
25. Zhuang, H.; Ding, J.; Chen, P.; Chang, Y.; Zeng, X.; Yang, H.; Liu, X.; Wei, W. Numerical Study on Static and Dynamic Performances of a Double-Pad Annular Inherently Compensated Aerostatic Thrust Bearing. *J. Tribol.* **2019**, *141*, 1–36, <https://doi.org/10.1115/1.4042657>.
26. Yang, J.; Rajasekar, S.; Sanjuán, M.A.F. Vibrational resonance: A review. *Physics Reports* **2024**, *1067*, 1–62.
27. Xia, H.; Zhang, N.; Guo, W. Analysis of resonance mechanism and conditions of train-bridge system. *J. Sound Vib.* **2006**, *297*, 810–822, <https://doi.org/10.1016/j.jsv.2006.04.022>.
28. Burda, E.A.; Zusman, G.V.; Kudryavtseva, I.S.; Naumenko, A.P.; Nicoletti, R. An Overview of Vibration Analysis Techniques for the Fault Diagnostics of Rolling Bearings in Machinery. *Shock. Vib.* **2022**, *2022*, 1–14, <https://doi.org/10.1155/2022/6136231>.
29. Yu, X.; Feng, Z.; Liang, M. Analytical vibration signal model and signature analysis in resonance region for planetary gearbox fault diagnosis. *J. Sound Vib.* **2021**, *498*, <https://doi.org/10.1016/j.jsv.2021.115962>.
30. Chu, T.; Nguyen, T.; Yoo, H.; Wang, J. A review of vibration analysis and its applications. *Heliyon* **2024**, *10*, e26282.
31. Li, W.; Zhu, C. Noncontact Rotor Vibration Velocity Sensor and Its Application to Vibration Control of a Flexible Rotor on Active Magnetic Bearings. *IEEE Sensors J.* **2024**, *24*, 34151–34161, <https://doi.org/10.1109/jsen.2024.3462482>.
32. Khan, S.A.; Kim, J.-M. Automated Bearing Fault Diagnosis Using 2D Analysis of Vibration Acceleration Signals under Variable Speed Conditions. *Shock. Vib.* **2016**, *2016*, 1–11, <https://doi.org/10.1155/2016/8729572>.
33. Hashad, A. Additional stresses on buildings induced by vibration effects. *Water Sci.* **2015**, *29*, 134–145, <https://doi.org/10.1016/j.wsj.2015.11.002>.
34. Dong, X.; Miao, Z.; Li, Y.; Zhou, H.; Li, W. One data-driven vibration acceleration prediction method for offshore wind turbine structures based on extreme gradient boosting. *Ocean Eng.* **2024**, *307*, <https://doi.org/10.1016/j.oceaneng.2024.118176>.
35. F, T.J. Piezoelectric sensors and sensor materials. *Journal of Electroceramics* **1998**, *2*, 257–272.
36. Habib, M.; Lantgios, I.; Hornbostel, K. A review of ceramic, polymer and composite piezoelectric materials. *Journal of Physics D: Applied Physics* **2022**, *55*, 423002.
37. Liang, X.; Cheng, W.; Li, S.; Hu, D.; Tan, Q. High-temperature shear-type vibration sensor based on langasite piezoelectric crystal. *Heliyon* **2024**, *10*, e38417, <https://doi.org/10.1016/j.heliyon.2024.e38417>.
38. Zhao, Z.; Wang, Z.; He, L.; Yokota, H.; Okada, Y.; Narita, F. Local impact sensing via flexible piezoelectric composite film based on highly elastic resin. *Sensors Actuators A: Phys.* **2024**, *368*, <https://doi.org/10.1016/j.sna.2024.115089>.
39. Promsawat, M.; Marungsri, B.; Promsawat, N.; Janphuang, P.; Luo, Z.; Pojprapai, S. Effects of temperature on aging degradation of soft and hard lead zirconate titanate ceramics. *Ceram. Int.* **2017**, *43*, 9709–9714, <https://doi.org/10.1016/j.ceramint.2017.04.145>.
40. Hao, J.; Li, W.; Zhai, J.; Chen, H. Progress in high-strain perovskite piezoelectric ceramics. *Mater. Sci. Eng. R: Rep.* **2019**, *135*, 1–57, <https://doi.org/10.1016/j.mser.2018.08.001>.
41. Wang, Q.; Liang, E.; Wang, C. High-performance bismuth titanate-ferrite (Bi5Ti3FeO15) for high-temperature piezoelectric applications. *Journal of the American Ceramic Society* **2024**, *107*, 4811–4823.

42. Sivagnanapalani, P.; Sahoo, B.; Panda, P. Calcium niobate based piezo-resistive materials for high temperature sensor application. *Ceram. Int.* **2018**, *44*, 20348–20353, <https://doi.org/10.1016/j.ceramint.2018.08.023>.
43. Zhang, L.S.; Bin Liu, Y.; Pan, C.L.; Feng, Z.H. Leakage current characterization and compensation for piezoelectric actuator with charge drive. *Sensors Actuators A: Phys.* **2013**, *199*, 116–122, <https://doi.org/10.1016/j.sna.2013.05.014>.
44. Ramany, K.; Shankararajan, R.; Savarimuthu, K.; Elumalai, P.; Rajamanickam, G.; Narendhiran, S.; Perumalsamy, R. Experimental Study of Different Vanadium Dopant Concentrations in ZnO Nanorods for a Low Frequency Piezoelectric Accelerometer. *J. Electron. Mater.* **2019**, *48*, 5310–5322, <https://doi.org/10.1007/s11664-019-07341-0>.
45. Ramanathan, A.K.; Headings, L.M.; Dapino, M.J. Near static strain measurement with piezoelectric films. *Sensors Actuators A: Phys.* **2020**, *301*, <https://doi.org/10.1016/j.sna.2019.111654>.
46. Ding, Y.; Wang, Y.; Liu, W.; Pan, Y.; Yang, P.; Meng, D.; Zheng, T.; Wu, J. Shear-structured piezoelectric accelerometers based on KNN lead-free ceramics for vibration monitoring. *J. Mater. Chem. C* **2024**, *12*, 18639–18650, <https://doi.org/10.1039/d4tc04292a>.
47. Deng, J.; Chuai, S.; Cai, Q.; An, D.; Shi, Y.; Shen, C.; Cao, H. Design and Preparation of Triaxial Piezoelectric Cryogenic Vibration Sensor Based on PZT-7A. *IEEE Sensors J.* **2024**, *25*, 2301–2309, <https://doi.org/10.1109/jsen.2024.3503602>.
48. Kinsler, P. Faraday's Law and Magnetic Induction: Cause and Effect, Experiment and Theory. *Physics* **2020**, *2*, 150–163, doi:10.3390/physics2020009.
49. Glynne-Jones, P.; Tudor, M.; Beeby, S.; White, N. An electromagnetic, vibration-powered generator for intelligent sensor systems. *Sensors Actuators A: Phys.* **2004**, *110*, 344–349, <https://doi.org/10.1016/j.sna.2003.09.045>.
50. Xue, X.; Dong, Y.; Wu, X. Motion Induced Eddy Current Sensor for Non-Intrusive Vibration Measurement. *IEEE Sensors J.* **2019**, *20*, 735–744, <https://doi.org/10.1109/jsen.2019.2943931>.
51. Ausanio, G.; Barone, A.; Hison, C.; Iannotti, V.; Luponio, C.; Lanotte, L. Mechanical vibration sensor based on elastomagnetic composite. *Sensors Actuators A: Phys.* **2006**, *129*, 25–28, <https://doi.org/10.1016/j.sna.2005.09.040>.
52. Xie, S.; Zhang, Y.; Jin, M.; Li, C.; Meng, Q. High Sensitivity and Wide Range Soft Magnetic Tactile Sensor Based on Electromagnetic Induction. *IEEE Sensors J.* **2020**, *21*, 2757–2766, <https://doi.org/10.1109/jsen.2020.3025830>.
53. Gurusamy, V.; Capolino, G.-A.; Akin, B.; Henao, H.; Romary, R.; Pusca, R. Recent Trends in Magnetic Sensors and Flux-Based Condition Monitoring of Electromagnetic Devices. *IEEE Trans. Ind. Appl.* **2022**, *58*, 4668–4684, <https://doi.org/10.1109/tia.2022.3174804>.
54. Shen, W.-A.; Zhu, S.; Xu, Y.-L. An experimental study on self-powered vibration control and monitoring system using electromagnetic TMD and wireless sensors. *Sensors Actuators A: Phys.* **2012**, *180*, 166–176, <https://doi.org/10.1016/j.sna.2012.04.011>.
55. Zhao, Y.; Gao, S.; Zhang, X.; Huo, W.; Xu, H.; Chen, C.; Li, J.; Xu, K.; Huang, X. Fully Flexible Electromagnetic Vibration Sensors with Annular Field Confinement Origami Magnetic Membranes. *Adv. Funct. Mater.* **2020**, *30*, <https://doi.org/10.1002/adfm.202001553>.
56. Butt, M.A.; Kazanskiy, N.L.; Khonina, S.N.; Voronkov, G.S.; Grakhova, E.P.; Kutluyarov, R.V. A Review on Photonic Sensing Technologies: Status and Outlook. *Biosensors* **2023**, *13*, 568, <https://doi.org/10.3390/bios13050568>.
57. Wampler, L.; Xia, F.; Yeung, S.Y.F.; Hirano, T.; Alshehri, A.H.; Furokawa, M.; Youcef-Toumi, K. A Doppler Radar With a Sweeping Lock-in Demodulator for Machine Vibration Sensing. *IEEE Sensors J.* **2023**, *23*, 28833–28844, <https://doi.org/10.1109/jsen.2023.3325820>.
58. Yang, X.; Li, X.; Meng, D.; Shi, J.; Miao, C. Optical fiber vibration sensor for bearing fault detection based on Sagnac interferometer. *Laser Phys.* **2023**, *33*, 065101, <https://doi.org/10.1088/1555-6611/acca04>.
59. Dejdard, P.; Mokry, O.; Cizek, M.; Rajmic, P.; Munster, P.; Schimmel, J.; Pravdova, L.; Horvath, T.; Cip, O. Characterization of sensitivity of optical fiber cables to acoustic vibrations. *Sci. Rep.* **2023**, *13*, 1–12, <https://doi.org/10.1038/s41598-023-34097-9>.

60. Huang, Z.; Nie, Z.; Xu, H.; Zhao, S.; Chen, G.; Hu, X.; Li, C.; Wang, G.; Li, D. A Multilongitudinal Mode Quadrature Laser Self-Mixing Vibration Sensor for Fault Diagnosis of Bearing. *IEEE Sensors J.* **2024**, *24*, 4407–4417, <https://doi.org/10.1109/jsen.2023.3348143>.
61. Li, Y.; Wang, Y.; Xiao, L.; Bai, Q.; Liu, X.; Gao, Y.; Zhang, H.; Jin, B. Phase Demodulation Methods for Optical Fiber Vibration Sensing System: A Review. *IEEE Sensors J.* **2021**, *22*, 1842–1866, <https://doi.org/10.1109/jsen.2021.3135909>.
62. Liu, K.; Jin, X.; Jiang, J.; Xu, T.; Ding, Z.; Huang, Y.; Sun, Z.; Xue, K.; Li, S.; Liu, T. Interferometer-Based Distributed Optical Fiber Sensors in Long-Distance Vibration Detection: A Review. *IEEE Sensors J.* **2022**, *22*, 21428–21444, <https://doi.org/10.1109/jsen.2022.3213036>.
63. Zhu, C.; Gerald, R.E.; Huang, J. Progress Toward Sapphire Optical Fiber Sensors for High-Temperature Applications. *IEEE Trans. Instrum. Meas.* **2020**, *69*, 8639–8655, <https://doi.org/10.1109/tim.2020.3024462>.
64. An, R.; Wang, Y.; Ping, X.; Wen, K.; Yuan, Y.; Wang, S.; Yang, J.; Wang, Y.; Qin, Y. Temperature Compensation Method for Polarization-Multiplexed Fiber-Optic Vibration Sensing Unit. *IEEE Sensors J.* **2024**, *25*, 2658–2666, <https://doi.org/10.1109/jsen.2024.3501256>.
65. Li, C.; Yang, W.; Wang, M.; Yu, X.; Fan, J.; Xiong, Y.; Yang, Y.; Li, L. A Review of Coating Materials Used to Improve the Performance of Optical Fiber Sensors. *Sensors* **2020**, *20*, 4215, <https://doi.org/10.3390/s20154215>.
66. Günther, P.; Pfister, T.; Büttner, L.; Czarske, J. Laser Doppler distance sensor using phase evaluation.. *Opt. Express* **2009**, *17*, 2611, <https://doi.org/10.1364/oe.17.002611>.
67. Chen, D.-M.; Zhu, W. Investigation of three-dimensional vibration measurement by a single scanning laser Doppler vibrometer. *J. Sound Vib.* **2017**, *387*, 36–52, <https://doi.org/10.1016/j.jsv.2016.09.026>.
68. Abbas, S.H.; Jang, J.-K.; Kim, D.-H.; Lee, J.-R. Underwater vibration analysis method for rotating propeller blades using laser Doppler vibrometer. *Opt. Lasers Eng.* **2020**, *132*, <https://doi.org/10.1016/j.optlaseng.2020.106133>.
69. Costanzo, A.; Falcone, S.; La Piana, C.; Lapenta, V.; Musacchio, M.; Sgamellotti, A.; Buongiorno, M.F. Laser Scanning Investigation and Geophysical Monitoring to Characterise Cultural Heritage Current State and Threat by Traffic-Induce Vibrations: The Villa Farnesina in Rome. *Remote. Sens.* **2022**, *14*, 5818, <https://doi.org/10.3390/rs14225818>.
70. Wu, X.; Xia, W.; Wang, X.; Song, H.; Huang, C. Effect of surface reflectivity on photonic Doppler velocimetry measurement. *Meas. Sci. Technol.* **2014**, *25*, <https://doi.org/10.1088/0957-0233/25/5/055207>.
71. Ho, J.; Jow, T.R.; Boggs, S. Historical introduction to capacitor technology. *IEEE Electr. Insul. Mag.* **2010**, *26*, 20–25, <https://doi.org/10.1109/mei.2010.5383924>.
72. K, B. MEMS capacitive accelerometers. *Sensor Letters* **2007**, *5*, 471–484.
73. Bakhoun, E.G.; Cheng, M.H.M. Ultrahigh-Sensitivity Pressure and Vibration Sensor. *IEEE Sensors J.* **2011**, *11*, 3288–3294, <https://doi.org/10.1109/jsen.2011.2155646>.
74. Nguyen, Q.-H.; Ngo, M.-Q.; Nguyen, D.-D.; Phan, N.-T.; Le, T.-T. Investigation of Parasitic Capacitance Models for Planar Transformers: Accuracy and Impedance Prediction. 2024 IEEE Applied Power Electronics Conference and Exposition (APEC). LOCATION OF CONFERENCE, United States DATE OF CONFERENCE; pp. 639–644.
75. Zhao, F.; Lei, B.; Jiang, W.; Jiang, W.; Lu, H.; Li, T.; Shi, Y.; Yin, L.; Chen, B.; Liu, H. The Intrinsic Mechanism of the Sensitivity Improvement for Capacitive Strain Sensors and Its Trade-Off With Sensing Range. *IEEE Sensors J.* **2023**, *24*, 4565–4573, <https://doi.org/10.1109/jsen.2023.3346196>.
76. Li, X.; Liang, Q.; Liu, H.; Zhao, L.; Sun, C.; Hou, C. High-Sensitivity MXene/MWCNTs/PDMS Flexible Capacitive Sensor for Wearable Health Monitoring. *Adv. Mater. Technol.* **2025**, <https://doi.org/10.1002/admt.202500677>.
77. Zhong, Y.; Liu, K.; Wu, L.; Ji, W.; Cheng, G.; Ding, J. Flexible Tactile Sensors with Gradient Conformal Dome Structures. *ACS Appl. Mater. Interfaces* **2024**, *16*, 52966–52976, <https://doi.org/10.1021/acsami.4c12736>.
78. Cheng, M.; Yuan, Y.; Li, Q.; Chen, C.; Chen, J.; Tian, K.; Zhang, M.; Fu, Q.; Deng, H. Polyimide aerogel-based capacitive pressure sensor with enhanced sensitivity and temperature resistance. *J. Mater. Sci. Technol.* **2024**, *217*, 60–69, <https://doi.org/10.1016/j.jmst.2024.08.015>.

79. Su, D.; Shen, G.; Ma, K.; Li, J.; Qin, B.; Wang, S.; Yang, W.; He, X. Enhanced sensitivity and linear-response in iontronic pressure sensors for non-contact, high-frequency vibration recognition. *J. Colloid Interface Sci.* **2024**, *659*, 1042–1051, <https://doi.org/10.1016/j.jcis.2023.12.181>.
80. Ghanam, M.; Goldschmidtboeing, F.; Bilger, T.; Bucherer, A.; Woias, P. MEMS Shielded Capacitive Pressure and Force Sensors with Excellent Thermal Stability and High Operating Temperature. *Sensors* **2023**, *23*, 4248, <https://doi.org/10.3390/s23094248>.
81. Qin, J.; Yin, L.; Hao, Y.; Zhong, S.; Zhang, D.; Bi, K.; Zhang, Y.; Zhao, Y.; Dang, Z. Flexible and Stretchable Capacitive Sensors with Different Microstructures. *Adv. Mater.* **2021**, *33*, 2008267, <https://doi.org/10.1002/adma.202008267>.
82. Ghemari, Z.; Belkhir, S.; Saad, S. A capacitive sensor with high measurement accuracy and low electrical energy consumption. *Appl. Phys. A* **2023**, *129*, 1–9, <https://doi.org/10.1007/s00339-023-06644-8>.
83. Gomathi, K.; Balaji, A.; Mrunalini, T. Design and optimization of differential capacitive micro accelerometer for vibration measurement. *J. Mech. Behav. Mater.* **2021**, *30*, 19–27, <https://doi.org/10.1515/jmbm-2021-0003>.
84. Do, C.; Seshia, A.A. Active Temperature Compensation for MEMS Capacitive Sensor. *IEEE Sensors J.* **2021**, *21*, 18588–18592, <https://doi.org/10.1109/jsen.2021.3089056>.
85. Li, C.; Sun, B.; Jia, P.; Xue, Y.; Jia, M.; Xiong, J. Capacitive Pressure Sensor With Integrated Signal-Conversion Circuit for High-Temperature Applications. *IEEE Access* **2020**, *8*, 212787–212793, <https://doi.org/10.1109/access.2020.3027951>.
86. Sui, Y.; Yu, T.; Wang, L.; Wang, Z.; Xue, K.; Chen, Y.; Liu, X.; Chen, Y. Analysis of a Capacitive Sensing Circuit and Sensitive Structure Based on a Low-Temperature-Drift Planar Transformer. *Sensors* **2022**, *22*, 9284, <https://doi.org/10.3390/s22239284>.
87. Augutis, V.; Balčiūnas, G.; Kuzas, P.; Gailius, D.; Raudienė, E. Smart Capacitive Transducer for High-Frequency Vibration Measurement. *Sensors* **2025**, *25*, 1639, <https://doi.org/10.3390/s25061639>.
88. Reverter, F. A Tutorial on Mechanical Sensors in the 70th Anniversary of the Piezoresistive Effect. *Sensors* **2024**, *24*, 3690, <https://doi.org/10.3390/s24113690>.
89. Barlian, A.A.; Park, W.-T.; Mallon, J.R.; Rastegar, A.J.; Pruitt, B.L. Review: Semiconductor Piezoresistance for Microsystems. *Proc. IEEE* **2009**, *97*, 513–552, <https://doi.org/10.1109/jproc.2009.2013612>.
90. Chung, D.D.L. A critical review of piezoresistivity and its application in electrical-resistance-based strain sensing. *J. Mater. Sci.* **2020**, *55*, 15367–15396, <https://doi.org/10.1007/s10853-020-05099-z>.
91. Irani, F.S.; Shafaghi, A.H.; Tasdelen, M.C.; Delipinar, T.; Kaya, C.E.; Yapici, G.G.; Yapici, M.K. Graphene as a Piezoresistive Material in Strain Sensing Applications. *Micromachines* **2022**, *13*, 119, <https://doi.org/10.3390/mi13010119>.
92. Zhang, D.; Xie, J.; Meng, X.; Pang, H.; Sun, R.; Fan, H.; Nan, X.; Zhou, Z. Development of piezoresistive flexible sensor with dual-height cylindrical microstructure surfaces to achieve vehicle vibration monitoring. *J. Micromechanics Microengineering* **2024**, *34*, 075005, <https://doi.org/10.1088/1361-6439/ad5564>.
93. Yuxiao, C.; Chunjun, C.; Chao, D. Research on Vibration Effect of Piezoresistive Pressure Sensor. *Instruments Exp. Tech.* **2022**, *65*, 653–667, <https://doi.org/10.1134/s0020441222040170>.
94. Tian, K.; Sui, G.; Yang, P.; Deng, H.; Fu, Q. Ultrasensitive Thin-Film Pressure Sensors with a Broad Dynamic Response Range and Excellent Versatility Toward Pressure, Vibration, Bending, and Temperature. *ACS Appl. Mater. Interfaces* **2020**, *12*, 20998–21008, <https://doi.org/10.1021/acsami.0c05618>.
95. Han, S.; Wu, Q.; Zhu, J.; Zhang, J.; Chen, A.; Chen, Y.; Yang, X.; Huang, J.; Guan, L. Multifunctional, superelastic, and environmentally stable sodium alginate/mxene/polydimethylsiloxane aerogels for piezoresistive sensor. *Chem. Eng. J.* **2023**, *471*, <https://doi.org/10.1016/j.cej.2023.144551>.
96. Yan, Y.; Zheng, J.; Zhang, Q.; Li, Y.; Li, G.; Zhang, Z.; Wang, P.; Wu, W.; Zhai, J.; Xu, Y. Ultrafast piezoresistive flexible pressure sensor for vibration and sound detection with a bandwidth over 20 kHz. *Chem. Eng. J.* **2025**, *517*, <https://doi.org/10.1016/j.cej.2025.164221>.
97. Tan, Z.; Hu, Q.-a.; Yang, B.; Liu, W.; Zhang, Z.; Shu, L.; Qiu, X. Superelastic and Highly Sensitive Biomass-Derived Piezoresistive Aerogels for Deep-Learning-Assisted Sensing. *Advanced Functional Materials* **2024**, *34*, e11831, <https://doi.org/10.1002/adfm.202411831>.
98. Wang, S.; Lin, L.; Wang, Z.L. Triboelectric nanogenerators as self-powered active sensors. *Nano Energy* **2015**, *11*, 436–462, <https://doi.org/10.1016/j.nanoen.2014.10.034>.

99. Niu, S.; Wang, Z.L. Theoretical systems of triboelectric nanogenerators. *Nano Energy* **2015**, *14*, 161–192, <https://doi.org/10.1016/j.nanoen.2014.11.034>.
100. Zhang, R.; Olin, H. Material choices for triboelectric nanogenerators: A critical review. *EcoMat* **2020**, *2*, <https://doi.org/10.1002/eom2.12062>.
101. Nguyen, V.; Yang, R. Effect of humidity and pressure on the triboelectric nanogenerator. *Nano Energy* **2013**, *2*, 604–608, <https://doi.org/10.1016/j.nanoen.2013.07.012>.
102. Zhang, J.; Boyer, C.; Zhang, Y.X. Enhancing the Humidity Resistance of Triboelectric Nanogenerators: A Review. *Small* **2024**, *20*, e2401846, <https://doi.org/10.1002/smll.202401846>.
103. Huang, Y.; Yu, H.; Xiao, Z.; Qin, M.; Mulvihill, D.M.; Zhang, Y.; Wang, Y.; Wen, J.; Jing, Q.; Cheng, Y. Self-powered wideband ultrasonic sensor based on capacitive triboelectric technology with ultralow detection limits and superior frequency resolution. *Nano Energy* **2025**, *141*, <https://doi.org/10.1016/j.nanoen.2025.111130>.
104. Mehamud, I.; Björling, M.; Marklund, P.; Shi, Y. Small Size and Low-Cost TENG-Based Self-Powered Vibration Measuring and Alerting System. *Advanced Electronic Materials* **2023**, *9*, 2300111.
105. Mousavi, M.; Alzgoool, M.; Davaji, B.; Towfighian, S. Event-driven MEMS vibration sensor: Integration of triboelectric nanogenerator and low-frequency switch. *Mech. Syst. Signal Process.* **2022**, *187*, <https://doi.org/10.1016/j.ymsp.2022.109921>.
106. Feng, P.; Yuan, Y.; Zhong, M.; Shao, J.; Liu, X.; Xu, J.; Zhang, J.; Li, K.; Zhao, W. Integrated Resistive-Capacitive Strain Sensors Based on Polymer–Nanoparticle Composites. *ACS Appl. Nano Mater.* **2020**, *3*, 4357–4366, <https://doi.org/10.1021/acsnm.0c00487>.
107. Shen, J.; Yang, Y.; Yang, Z.; Li, B.; Ji, L.; Cheng, J. A multilayer triboelectric-electromagnetic hybrid nanogenerator for vibration energy harvesting and frequency monitoring. *Nano Energy* **2023**, *116*, <https://doi.org/10.1016/j.nanoen.2023.108818>.
108. Wu, H.; Wang, Z.; Zhu, B.; Wang, H.; Lu, C.; Kang, M.; Kang, S.; Ding, W.; Yang, L.; Liao, R.; et al. All-in-One Sensing System for Online Vibration Monitoring via IR Wireless Communication as Driven by High-Power TENG. *Adv. Energy Mater.* **2023**, *13*, <https://doi.org/10.1002/aenm.202300051>.
109. Zhang, D.; Zhang, R.; Zhao, Q.; He, H.; Huang, H.; Yang, L.; Xu, Y. High-linearity flexible sensor for real-time pressure monitoring across wide frequency range by integrating piezoelectric and piezoresistive effects. *Chem. Eng. J.* **2025**, *506*, <https://doi.org/10.1016/j.cej.2025.159919>.
110. Wang, L.; Fei, Z.; Duan, C.; Han, X.; Li, M.; Gao, W.; Xia, Y.; Jia, C.; Lin, Q.; Zhao, Y.; et al. Self-sustained and self-wakeup wireless vibration sensors by electromagnetic-piezoelectric-triboelectric hybrid energy harvesting. *Appl. Energy* **2023**, *355*, <https://doi.org/10.1016/j.apenergy.2023.122207>.
111. Wang, A.; Gao, Z.; Wu, S.; Wei, Y.; Lu, B.; Shi, J.; Shen, L.; Liu, Y.; Sun, X.; Wen, Z. Superelastic and Ultra-Soft MXene/CNF Aerogel@PDMS-Based Dual-Modal Pressure Sensor for Complex Stimuli Monitoring. *Adv. Sci.* **2025**, *12*, e2502797, <https://doi.org/10.1002/advs.202502797>.
112. Malla, C.; Panigrahi, I. Review of Condition Monitoring of Rolling Element Bearing Using Vibration Analysis and Other Techniques. *J. Vib. Eng. Technol.* **2019**, *7*, 407–414, <https://doi.org/10.1007/s42417-019-00119-y>.
113. Kibrete, F.; Woldemichael, D.E.; Gebremedhen, H.S. Multi-Sensor data fusion in intelligent fault diagnosis of rotating machines: A comprehensive review. *Measurement* **2024**, *232*, <https://doi.org/10.1016/j.measurement.2024.114658>.
114. Zaitsev, I.; Bereznychenko, V.; Bajaj, M.; Taha, I.B.M.; Belkhier, Y.; Titko, V.; Kamel, S. Calculation of Capacitive-Based Sensors of Rotating Shaft Vibration for Fault Diagnostic Systems of Powerful Generators. *Sensors* **2022**, *22*, 1634, <https://doi.org/10.3390/s22041634>.
115. Hu, Y.; Guo, R.; Wang, H.; Zhao, R.; Ning, R.; Huang, Z.; Chu, Z.; Peng, Y.; Zhang, Y.; Zhang, H. Gear-fault monitoring and digital twin demonstration of aircraft engine based on piezoelectric vibration sensor for engine health management. *Nano Energy* **2024**, *133*, <https://doi.org/10.1016/j.nanoen.2024.110448>.
116. Pawlenka, T.; Škuta, J.; Tůma, J.; Juránek, M. Development of capacitive sensors for measuring vibrations and small displacements of a high-speed rotating machines for use in active vibration control systems. *Sensors Actuators A: Phys.* **2023**, *365*, <https://doi.org/10.1016/j.sna.2023.114902>.

117. Papathanasopoulos, D.A.; Giannousakis, K.N.; Dermatas, E.S.; Mitronikas, E.D. Vibration Monitoring for Position Sensor Fault Diagnosis in Brushless DC Motor Drives. *Energies* **2021**, *14*, 2248, <https://doi.org/10.3390/en14082248>.
118. Goyal, D.; Pabla, B.S. The Vibration Monitoring Methods and Signal Processing Techniques for Structural Health Monitoring: A Review. *Arch. Comput. Methods Eng.* **2015**, *23*, 585–594, <https://doi.org/10.1007/s11831-015-9145-0>.
119. Salawu, O. Detection of structural damage through changes in frequency: a review. *Eng. Struct.* **1997**, *19*, 718–723, [https://doi.org/10.1016/s0141-0296\(96\)00149-6](https://doi.org/10.1016/s0141-0296(96)00149-6).
120. Lieven, N.A.J.; Ewins, D.J.; Farrar, C.R.; Doebling, S.W.; Nix, D.A. Vibration-based structural damage identification. *Philosophical Transactions of the Royal Society of London. Series A: Mathematical, Physical and Engineering Sciences* **2001**, *359*, 131-149.
121. Lin, Z.; Sun, C.; Liu, W.; Fan, E.; Zhang, G.; Tan, X.; Shen, Z.; Qiu, J.; Yang, J. A self-powered and high-frequency vibration sensor with layer-powder-layer structure for structural health monitoring. *Nano Energy* **2021**, *90*, <https://doi.org/10.1016/j.nanoen.2021.106366>.
122. Mustapha, S.; Lu, Y.; Ng, C.-T.; Malinowski, P. Sensor Networks for Structures Health Monitoring: Placement, Implementations, and Challenges—A Review. *Vibration* **2021**, *4*, 551–585, <https://doi.org/10.3390/vibration4030033>.
123. Li, X.; Guan, Y.; Law, S.; Zhao, W. Monitoring abnormal vibration and structural health conditions of an in-service structure from its SHM data. *J. Sound Vib.* **2022**, *537*, 109175. <https://doi.org/10.1016/j.jsv.2022.117185>.
124. Zhang, M.; Guo, T.; Zhu, R.; Zong, Y.; Liu, Z.; Xu, W. Damage identification of seismic-isolated structure based on CAE network using vibration monitoring data. *Eng. Struct.* **2023**, *283*, <https://doi.org/10.1016/j.engstruct.2023.115873>.
125. Cui, J.; Li, X.; Wang, K.; Yan, X.; Zheng, Y.; Xue, C. A wide-frequency triboelectric vibration sensor for self-powered machinery health monitoring. *Nano Energy* **2024**, *133*, <https://doi.org/10.1016/j.nanoen.2024.110481>.
126. Muxica, D.; Rivera, S.; Orchard, M.E.; Ahumada, C.; Jaramillo, F.; Bravo, F.; Gutiérrez, J.M.; Astroza, R. Autonomous Sensor System for Low-Capacity Wind Turbine Blade Vibration Measurement. *Sensors* **2024**, *24*, 1733, <https://doi.org/10.3390/s24061733>.
127. Xiong, Q.; Tang, J.; Ding, T.; Wang, A.; Yu, X.; Zhang, W.; Bai, X. Dynamic Modeling and Vibration Response Analysis of Rolling Bearings With Composite Faults Considering the Influence of Elastohydrodynamic Lubrication. *Shock. Vib.* **2024**, *2024*, <https://doi.org/10.1155/vib/1057592>.
128. Chen, Q.; Cen, J.; Chen, K.; Zhang, X.; Feng, C.; Zhang, D.; Ge, S. Evolution behavior on friction-induced vibration and lubrication state identification. *Tribol. Int.* **2025**, *210*, <https://doi.org/10.1016/j.triboint.2025.110817>.
129. Cao, L.; Li, X.; Wang, Q.; Zhang, D. Vibration analysis and numerical simulation of rolling interface during cold rolling with unsteady lubrication. *Tribol. Int.* **2021**, *153*, <https://doi.org/10.1016/j.triboint.2020.106604>.
130. Hou, G.; Zhang, L. In-situ detection of lubrication status of bearings with acoustic emission monitoring. *Wear* **2025**, *571*, <https://doi.org/10.1016/j.wear.2025.205839>.
131. Long, R.; Sun, Y.; Zhang, Y.; Shang, Q.; Ramteke, S.M.; Marian, M. Influence of micro-texture radial depth variations on the tribological and vibration characteristics of rolling bearings under starved lubrication. *Tribol. Int.* **2024**, *194*, <https://doi.org/10.1016/j.triboint.2024.109545>.
132. Liu, Q.; Ouyang, W.; Li, R.; Jin, Y.; He, T. Experimental research on lubrication and vibration characteristics of water-lubricated stern bearing for underwater vehicles under extreme working conditions. *Wear* **2023**, *523*, <https://doi.org/10.1016/j.wear.2023.204778>.
133. Chen, Y.; Zhang, H.; Li, X.; Xiao, S.; Gu, F.; Shi, Z. Effects of Wear on Lubrication Performance and Vibration Signatures of Rotor System Supported by Hydrodynamic Bearings. *Lubricants* **2023**, *11*, 107, <https://doi.org/10.3390/lubricants11030107>.
134. Zhang, K.; Wu, X.; Bai, X.; Wang, Z.; Zou, D.; Sun, J. Effect of the Lubrication Parameters on the Ceramic Ball Bearing Vibration in Starved Conditions. *Appl. Sci.* **2020**, *10*, 1237, <https://doi.org/10.3390/app10041237>.

135. Akhlaghi, M.A.; Bagherpour, R.; Hoseinie, S.H. Real-time monitoring of disc cutter wear in tunnel boring machines: A sound and vibration sensor-based approach with machine learning technique. *J. Rock Mech. Geotech. Eng.* **2024**, *17*, 1700–1722, <https://doi.org/10.1016/j.jrmge.2024.04.030>.
136. Wan, L.; Chen, Z.; Zhang, X.; Wen, D.; Ran, X. A multi-sensor monitoring methodology for grinding wheel wear evaluation based on INFO-SVM. *Mech. Syst. Signal Process.* **2023**, *208*, <https://doi.org/10.1016/j.ymsp.2023.111003>.
137. Wang, Y.; Liu, T.; Luo, D.; Du, Z.; Yao, L.; Zhang, Y. Study on the tribological and tribo-vibration characteristics of laser textured tapered roller bearings under full oil lubrication. *Ind. Lubr. Tribol.* **2024**, *77*, 281–290, <https://doi.org/10.1108/ilt-09-2024-0357>.
138. Wu, Y.; Guo, J.; Zhang, X.; Zhou, P.; Meng, W.; Bai, X.; Lu, H. Vibration properties of full ceramic bearing under elasto-hydrodynamic fluid lubrication based on the energy approach. *Case Stud. Therm. Eng.* **2024**, *64*, <https://doi.org/10.1016/j.csite.2024.105459>.
139. Chen, H.-Y.; Lee, C.-H. Vibration Signals Analysis by Explainable Artificial Intelligence (XAI) Approach: Application on Bearing Faults Diagnosis. *IEEE Access* **2020**, *8*, 134246–134256, <https://doi.org/10.1109/access.2020.3006491>.
140. Zhang, P.; Gao, D.; Lu, Y.; Ma, Z.; Wang, X.; Song, X. Cutting tool wear monitoring based on a smart toolholder with embedded force and vibration sensors and an improved residual network. *Measurement* **2022**, *199*, <https://doi.org/10.1016/j.measurement.2022.111520>.
141. Sayyad, S.; Kumar, S.; Bongale, A.; Kamat, P.; Patil, S.; Kotecha, K. Data-Driven Remaining Useful Life Estimation for Milling Process: Sensors, Algorithms, Datasets, and Future Directions. *IEEE Access* **2021**, *9*, 110255–110286, <https://doi.org/10.1109/access.2021.3101284>.
142. Wang, Y.; Zheng, L.; Gao, Y.; Li, S. Vibration Signal Extraction Based on FFT and Least Square Method. *IEEE Access* **2020**, *8*, 224092–224107, <https://doi.org/10.1109/access.2020.3044149>.
143. Brusa, E.; Bruzzone, F.; Delprete, C.; Di Maggio, L.G.; Rosso, C. Health Indicators Construction for Damage Level Assessment in Bearing Diagnostics: A Proposal of an Energetic Approach Based on Envelope Analysis. *Appl. Sci.* **2020**, *10*, 8131, <https://doi.org/10.3390/app10228131>.
144. Thoppil, N.M.; Vasu, V.; Rao, C.S.P. Health indicator construction and remaining useful life estimation for mechanical systems using vibration signal prognostics. *Int. J. Syst. Assur. Eng. Manag.* **2021**, *12*, 1001–1010, <https://doi.org/10.1007/s13198-021-01190-z>.
145. Wang, Y., Zhao, Y., Addepalli, S. Remaining useful life prediction using deep learning approaches: A review. In: *Procedia Manufacturing*. pp. 81–88. Elsevier B.V. (2020)
146. Ferreira, C.; Gonçalves, G. Remaining Useful Life prediction and challenges: A literature review on the use of Machine Learning Methods. *J. Manuf. Syst.* **2022**, *63*, 550–562, <https://doi.org/10.1016/j.jmsy.2022.05.010>.
147. Fu, C.; Gao, C.; Zhang, W. A Digital-Twin Framework for Predicting the Remaining Useful Life of Piezoelectric Vibration Sensors with Sensitivity Degradation Modeling. *Sensors* **2023**, *23*, 8173, <https://doi.org/10.3390/s23198173>.
148. Guo, J.; Wan, J.-L.; Yang, Y.; Dai, L.; Tang, A.; Huang, B.; Zhang, F.; Li, H. A deep feature learning method for remaining useful life prediction of drilling pumps. *Energy* **2023**, *282*, <https://doi.org/10.1016/j.energy.2023.128442>.
149. Yu, L.; Qiao, Z.; Xing, S.; Wu, Y.; Ji, H. A Novel Structural Vibration Sensing Approach Based on a Miniaturized Inertial Measurement Unit. *Sensors* **2025**, *25*, 3958, <https://doi.org/10.3390/s25133958>.
150. Hong, L.; Wu, X.; Gao, Q.; Pei, C.; Liu, K. A study on double-cantilever miniaturized FBG acceleration sensors for low-frequency vibration monitoring. *J. Opt.* **2023**, *53*, 1282–1292, <https://doi.org/10.1007/s12596-023-01294-8>.
151. Li, P.; Feng, Y.; Ding, C.; Zhong, R.; Yan, W.; Song, J.; Hong, Z.; Hu, B.; Tan, J.; Sun, J.; et al. Magnetointeractive Cr₂Te₃-Coated Liquid Metal Droplets for Flexible Memory Arrays and Wearable Sensors. *Advanced Materials* **2025**, *37*, 2414519.
152. Bhatta, T.; Faruk, O.; Islam, M.R.; Kim, H.S.; Rana, S.S.; Pradhan, G.B.; Deo, A.; Kwon, D.-S.; Yoo, I.; Park, J.Y. Polymeric multilayered planar spring-based hybrid nanogenerator integrated with a self-powered vibration sensor for automotive vehicles IoT applications. *Nano Energy* **2024**, *127*, <https://doi.org/10.1016/j.nanoen.2024.109793>.

153. Tang, M.; Fang, Z.; Fan, C.; Zhang, Z.; Kong, L.; Chen, H.; Zeng, Z.; Yang, Y.; Qi, L. An AI-driven electromagnetic-triboelectric self-powered and vibration-sensing system for smart transportation. *Eng. Struct.* **2024**, *323*, <https://doi.org/10.1016/j.engstruct.2024.119275>.
154. Lin, H.; Liu, D.; Zhou, Y.; Liu, M.; Huang, C.; Fu, Q.; Deng, K.; Huang, Y.; Huang, X.; Zhang, P.; et al. A flexible PTI-CNT strain sensor with high stretchable and sensitive for human movement and vocal cord vibration monitoring. *Polymer* **2024**, *299*, <https://doi.org/10.1016/j.polymer.2024.126887>.
155. Wang, Z.; Zhou, W.; Xiao, Z.; Yao, Q.; Xia, X.; Mei, J.; Zhang, D.; Chen, P.; Li, S.; Wang, Y.; et al. A High-Temperature Accelerometer with Excellent Performance Based on the Improved Graphene Aerogel. *ACS Appl. Mater. Interfaces* **2023**, *15*, 19337–19348, <https://doi.org/10.1021/acsami.3c00418>.
156. Li, A.; Xu, J.; Xu, D.; Zhang, Z.; Cao, D.; Li, J.; Zhang, W.; Zhang, F. High-performance, breathable, and degradable fully cellulose-based sensor for multifunctional human activity monitoring. *Chem. Eng. J.* **2025**, *505*, <https://doi.org/10.1016/j.cej.2025.159564>.
157. Philibert, M.; Yousry, Y.M.; Wong, V.-K.; Yao, K. Ultrasonic Surface Wave Transducers Made of Piezoelectric Polylactic Acid for Structural Health Monitoring. *IEEE Sensors J.* **2024**, *24*, 29770–29777, <https://doi.org/10.1109/jsen.2024.3442307>.
158. Zhu, K.; Yang, S.; Jiang, H.; He, Y.; Chen, Z.; Zhang, B.; Zhang, Q.; Zhang, H. A robust biomass superhydrophobic sensor for Re-healing and underwater vibration detection. *Carbon* **2023**, *218*, <https://doi.org/10.1016/j.carbon.2023.118770>.
159. Chai, B.; Shi, K.; Wang, Y.; Liu, Y.; Liu, F.; Zhu, L.; Huang, X. Integrated Piezoelectric/Pyroelectric Sensing from Organic–Inorganic Perovskite Nanocomposites. *ACS Nano* **2024**, *18*, 25216–25225, <https://doi.org/10.1021/acsnano.4c07480>.
160. Xie, M.; Qian, G.; Yu, Y.; Chen, C.; Li, H.; Li, D. High-performance flexible reduced graphene oxide/polyimide nanocomposite aerogels fabricated by double crosslinking strategy for piezoresistive sensor application. *Chem. Eng. J.* **2023**, *480*, <https://doi.org/10.1016/j.cej.2023.148203>.
161. Wu, G.; Li, X.; Bao, R.; Pan, C. Innovations in Tactile Sensing: Microstructural Designs for Superior Flexible Sensor Performance. *Adv. Funct. Mater.* **2024**, *34*, <https://doi.org/10.1002/adfm.202405722>.
162. Liu, J.; Zhang, X.; Liu, J.; Liu, X.; Zhang, C. 3D Printing of Anisotropic Piezoresistive Pressure Sensors for Directional Force Perception. *Adv. Sci.* **2024**, *11*, e2309607, <https://doi.org/10.1002/advs.202309607>.
163. Zhang, L.; Bian, Y.; Wei, W.; Liao, Z.; Cang, M.; Yang, A.; Zhi, H.; Zhang, W.; Chen, M.; Cui, H.; et al. Dendrite-Inspired and 3D Printed Multidirectional Sensing Piezoresistive Metamaterials. *Adv. Funct. Mater.* **2025**, <https://doi.org/10.1002/adfm.202508987>.
164. Qin, L.; Zhang, L.; Feng, J.; Zhang, F.; Han, Q.; Qin, Z.; Chu, F. A hybrid triboelectric-piezoelectric smart squirrel cage with self-sensing and self-powering capabilities. *Nano Energy* **2024**, *124*, <https://doi.org/10.1016/j.nanoen.2024.109506>.
165. Su, C.; Jia, P.; Zhao, A.; Tu, J.; Liu, J.; Ren, Q.; Xiong, J. Temperature-Decoupled Single-Crystal MgO Fiber-Optic Fabry–Perot Vibration Sensor Based on MEMS Technology for Harsh Environments. *Micromachines* **2024**, *15*, 616, <https://doi.org/10.3390/mi15050616>.
166. Hsu, C.-Y.; Chen, P.-H.; Chen, T.-Y.; Lin, S.-Y.; Wang, C.-J.; Yeh, C.; Lin, T.-J.; Chang, P.-Z.; Li, W.-C. Performance Evaluation of MEMS Vibration Sensors for Throat Microphones. 2024 IEEE SENSORS. LOCATION OF CONFERENCE, JapanDATE OF CONFERENCE; pp. 1–4.
167. Signore, M.; De Pascali, C.; Quaranta, F.; Velardi, L.; Valerini, D.; Farella, I.; Di Gloria, P.; De Giorgi, M.; Ficarella, A.; Francioso, L. Fabrication and characterization of a piezo-MEMS uniaxial accelerometer as a tool for the monitoring of combustion instability in gas turbine engines. *Measurement* **2025**, *256*, <https://doi.org/10.1016/j.measurement.2025.118166>.
168. Zhang, M.; Xing, X.; Wang, W. Smart Sensor-Based Monitoring Technology for Machinery Fault Detection. *Sensors* **2024**, *24*, 2470, <https://doi.org/10.3390/s24082470>.
169. Zhang, Z.; Lombardo, L.; Shi, T.; Han, X.; Parvis, M.; Li, J. A smart combined wireless sensor for vibration and AE signals measurement. In Proceedings of the 2024 IEEE International Instrumentation and Measurement Technology Conference (I2MTC), 20-23 May 2024.

Disclaimer/Publisher's Note: The statements, opinions and data contained in all publications are solely those of the individual author(s) and contributor(s) and not of MDPI and/or the editor(s). MDPI and/or the editor(s) disclaim responsibility for any injury to people or property resulting from any ideas, methods, instructions or products referred to in the content.